



doi:10.1016/j.gca.2003.10.009

## The Hadean upper mantle conundrum: Evidence for source depletion and enrichment from Sm-Nd, Re-Os, and Pb isotopic compositions in 3.71 Gy boninite-like metabasalts from the Isua Supracrustal Belt, Greenland

ROBERT FREI,<sup>1,\*</sup> ALI POLAT,<sup>2</sup> and ANDERS MEIBOM<sup>3</sup><sup>1</sup>Geological Institute, University of Copenhagen, Øster Voldgade 10, DK-1350 Copenhagen K, Denmark<sup>2</sup>Department of Earth Sciences, University of Windsor, Windsor, Ontario N9B 3P4, Canada<sup>3</sup>Geological and Environmental Sciences, 320 Lomita Mall, Stanford University, Stanford, CA 94305, USA

(Received July 23, 2003; accepted in revised form October 15, 2003)

**Abstract**—Here we present Sm-Nd, Re-Os, and Pb isotopic data of carefully screened, least altered samples of boninite-like metabasalts from the Isua Supracrustal Belt (ISB, W Greenland) that characterize their mantle source at the time of their formation. The principal observations of this study are that by 3.7–3.8 Ga melt source regions existed in the upper mantle with complicated enrichment/depletion histories. Sm-Nd isotopic data define a correlation line with a slope corresponding to an age of  $3.69 \pm 0.18$  Gy and an initial  $\epsilon_{\text{Nd}}$  value of  $+2.0 \pm 4.7$ . This Sm-Nd age is consistent with indirect (but more precise) U-Pb geochronological estimates for their formation between 3.69–3.71 Ga. Relying on the maximum formation age of 3.71 Gy defined by the external age constraints, we calculate an average  $\epsilon_{\text{Nd}}$  [T = 3.71 Ga] value of  $+2.2 \pm 0.9$  (n = 18, 1 $\sigma$ ) for these samples, which is indicative of a strongly depleted mantle source. This is consistent with the high Os concentrations, falling in the range between 1.9–3.4 ppb, which is similar to the estimated Os concentration for the primitive upper mantle. Re-Os isotopic data (excluding three outliers) yield an isochron defining an age of  $3.76 \pm 0.09$  Gy (with an initial  $\gamma_{\text{Os}}$  value of  $3.9 \pm 1.2$ ), within error consistent with the Sm-Nd age and the indirect U-Pb age estimates. An average initial  $\gamma_{\text{Os}}$  [T = 3.71 Ga] value of  $+4.4 \pm 1.2$  (n = 8; 2 $\sigma$ ) is indicative of enrichment of their source region during, or prior to, its melting. Thus, this study provides the first observation of an early Archean upper mantle domain with a distinctly radiogenic Os isotopic signature. This requires a mixing component characterized by time-integrated suprachondritic Re/Os evolution and a Os concentration high enough to strongly affect the Os budget of the mantle source; modern sediments, recycled basaltic crust, or the outer core do not constitute suitable candidates. At this point, the nature of the mantle or crustal component responsible for the radiogenic Os isotopic signature is not known.

Compared with the Sm-Nd and Re-Os isotope systems, the Pb isotope systematics show evidence for substantial perturbation by postformational hydrothermal-metasomatic alteration processes accompanying an early Archean metamorphic event at  $3510 \pm 65$  Ma and indicate that the U-Th-Pb system was partially opened to Pb-loss on a whole rock scale. Single stage mantle evolution models fail to provide a solution to the Pb isotopic data, which requires that a high- $\mu$  component was mixed with the depleted mantle component before or during the extrusion of the basalts. Relatively high  $^{207}\text{Pb}/^{204}\text{Pb}$  ratios (compared to contemporaneous mantle), support the hypothesis that erosion products of the ancient terrestrial protocrust existed for several hundred My before recycling into the mantle before  $\sim 3.7$  Ga.

Our results are broadly consistent with models favoring a time-integrated Hadean history of mantle depletion and with the existence of an early Hadean protocrust, the complement to the Hadean depleted mantle, which after establishment of subduction-like processes was, at least locally, recycled into the upper mantle before 3.7 Ga. Thus, already in the Hadean, the upper mantle seems to be characterized by geochemical heterogeneity on a range of length scales; one property that is shared with the modern upper mantle. However, a simple two component mixing scenario between depleted mantle and an enriched-, crustal component with a modern analogue can not account for the complicated and contradictory geochemical properties of this particular Hadean upper mantle source. Copyright © 2004 Elsevier Ltd

### 1. INTRODUCTION

The geochemical study of modern, Phanerozoic (ophiolite-associated) and Archean (greenstone belt-hosted) mafic to ultramafic volcanic rocks has resulted in an increased understanding of the complex mechanisms of depletion and enrichment processes within their upper mantle sources through time (e.g., Sun, 1987; Jochum et al., 1991; Arndt et al., 1997; Puchtel et al., 1998; and many others). However, the scarcity of

Hadean/Early Archean rocks and the effects of metamorphism and associated hydrothermal-metasomatic processes limits the degree to which major, trace element and isotopic data constrain the geochemical nature of the Earth's earliest crust-mantle system. Isotope systems, such as Sm-Nd, Lu-Hf, Re-Os and U-Pb are often applied to investigate the behavior of lithophile and siderophile elements in the evolution of the crust-mantle system. But, the precise calculation of initial isotopic ratios that can characterize the different mantle source regions is problematic, especially for the Hadean–Early Archean. This is because, despite the long half-lives of these isotope systems, on such long time scales the radiogenic in-

\* Author to whom correspondence should be addressed (robertf@geo.geol.ku.dk).

growth of their daughter products render the determination of initial isotope ratios vulnerable to postformational alteration of the parent-daughter ratios and sensitive to in situ age correction. A combination of several isotopic systems, including both lithophile and siderophile elements, can potentially remove some of these obstacles (Carlson and Irving, 1994) and lead to improved, or better constrained geochemical interpretations of the often complex depletion/enrichment histories of the basaltic source regions in the upper mantle through time.

The aim of this study is to expand upon the previously published geochemical data on a suite of carefully selected (screened for minimum alteration of their trace elements) samples of high-Mg, low-High Field Strength Element (HFSE) (boninite-like) metabasalts with subduction enrichment geochemical signatures from within the Isua Supracrustal Belt (ISB). The combined Sm-Nd, Re-Os, and Pb isotope systematics presented here help to further characterize their mantle source and to gain additional insights into their petrogenesis.

## 2. GEOLOGICAL FRAMEWORK AND ALTERATION HISTORY

The ISB is primarily composed of two major packages of volcanic to volcano-sedimentary sequences. In the SW, W and northeast part of the ISB, volcanics from within a central tectonic domain can be geochemically and geochronologically distinguished from those belonging to an inner and outer tectonic zone. In the northeast part of the ISB (Fig. 1), the central tectonic domain is larger than metavolcanics found in the outer and inner tectonic zones. The geochemical characteristics of the metavolcanic rocks from the central and the inner/outer tectonic domains were discussed by Polat et al. (2002a) and Polat and Hofmann (2003). On the basis of the least mobile elements in samples screened for minimum alteration, metavolcanics from the central lithotectonic domain define a low-HFSE volcanic association, whereas the outer and inner tectonic zones comprise high-HFSE metavolcanic suites. Both suites span a continuous ultramafic to mafic compositional range, consistent with olivine-controlled fractionation processes. The low-HFSE volcanic suite was determined to be “boninitic” by Polat et al. (2002a) because of its geochemical similarity to those of Tertiary boninites from arcs of the western Pacific Ocean. The high-HFSE association has geochemical features similar to those of Tertiary oceanic island arc basaltic to picritic lavas (Polat and Hofmann, 2003).

The suite from the central tectonic domain (also referred to as the “Garbenschiefer Unit” due to the prevalence of garben-textured hornblende) is comprised of a succession of basaltic lavas, interstratified volcano-sedimentary horizons, interbedded banded iron formations (BIF) and other sedimentary units (Rosing et al., 1996). The inner and outer arc sequences are dominated by amphibolites (also referred to as the “Amphibolite Unit”), and both contain lenses of variably metasomatized ultramafic rocks. A number of low-strain zones within the “Amphibolite Unit” and “Garbenschiefer Unit” contain well-preserved pillowed metabasalts. Maruyama et al. (1992) and Komiya and Maruyama (1995) first proposed modern oceanic basalt analogs for these sequences and more detailed primary volcanic features of the metabasalts from the central tectonic domain of the northeast part of the ISB have been later de-

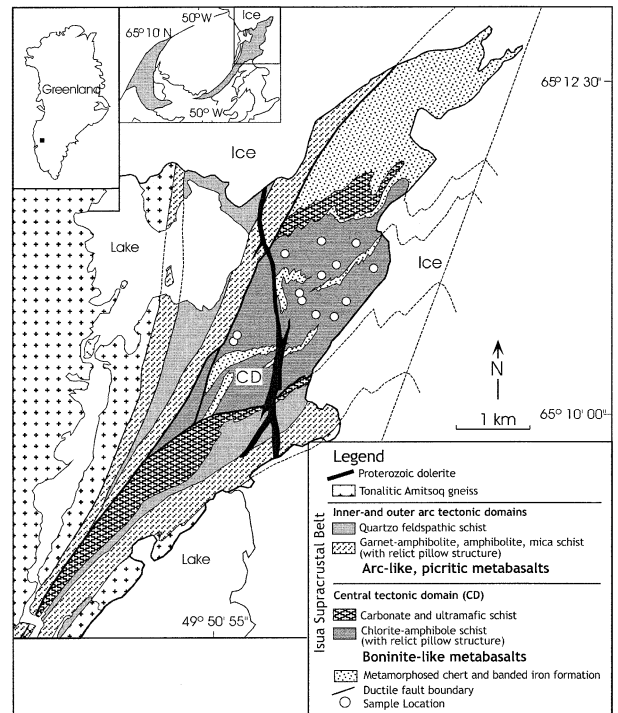


Fig. 1. Map of the northeast part of the ISB (modified from Polat et al., 2002a) with sample locations of boninite-like metabasalts used in this study. The samples were collected from within a low-strain zone of the central tectonic domain dominated by chlorite-amphibole schists, also called garbenschiefer due to their garben-textured hornblende, where metasomatic alteration and metamorphic overprinting are minimal. Genetically associated BIF occur to the northeast of the sample area.

scribed in detail by Appel et al. (1998), Polat et al. (2002a) and Polat and Hofmann (2003).

Sheets of gray gneisses (meta-tonalites) are found to intrude the metavolcanics from the inner and outer-, but not from the central lithotectonic domains. SHRIMP U-Pb ages of 3.79–3.81 Gy (Nutman et al., 1997; Nutman et al., 2002) on zircons from a number of such tonalite sheets have led to the suggestion that the volcanic association from the inner and outer tectonic domain may represent an older volcanic suite formed more than 3.79 Ga. The lack of such tonalite sheets in the apparently ~3.71 Ga old “Garbenschiefer Unit” led Nutman et al. (1997, 2002) and to postulate a tectonic juxtaposition of the two units after the intrusion of the gray gneisses, but before regional, 3.56–3.58 Gy old, thermal events that are recorded by metamorphic zircon growth throughout the area (Nutman et al., 2002).

The “Amphibolite Unit” and “Garbenschiefer Unit” rocks in the W and NW sector were affected by massive infiltration metasomatism (Rose et al., 1996; Rosing et al., 1996; Blichert-Toft et al., 1999; Frei et al., 2002). Based on field evidence, alteration took place during and after the penetrative regional amphibolite metamorphism and accompanying deformation, and after the intrusion of the tonalite gneiss sheets. Metasomatic reactions are mainly characterized by desilication and formation of calc-silicates restricted to the contacts between ultramafic lenses and their country rocks, and by subsequent

localized carbonation and K-metasomatism (Rosing et al., 1996).

Based on the combination of initial Pb isotopic constraints of hydrothermal-metasomatic galena and of 3.74 Ga Pb-Pb mineral ages, Frei and Rosing (2001) concluded that there is a close genetic relationship between early Archean fluid flow and the earliest magmatic events.

Previous studies (e.g., Shimizu et al., 1990; Gruau et al., 1996; Frei et al., 1999a,b; Rosing and Frei, 1999; Frei and Rosing, 2001) indicated that the “Garbenschiefer Unit” and the “Amphibolite Unit” in the W and SW sectors of the ISB were tectono-metamorphically overprinted ca. 2.6–2.85 Gy ago. This is consistent with the late Archean partial and full resetting of the U-Pb system in titanite and apatite, respectively, in the tonalite gneisses to the south of the ISB (Baadsgaard, 1983).

Finally, regional heating to greenschist facies conditions took place during the Paleoproterozoic. This is reflected in the resetting of low temperature geochronometers, such as the Rb-Sr isotopic system in biotite from tonalitic gneisses in the Isua area (Baadsgaard et al., 1986), which consistently yield cooling ages of ca. 1.6–1.7 Ga.

Postformational alteration processes are mainly related to metamorphic and metasomatic processes in conjunction with intrusion of granitoids at various times in the early and possibly late Archean (Gruau et al., 1996; Rosing et al., 1996; Frei et al., 1997; Appel et al., 1998; Frei et al., 2002; Myers, 2002 and others). Recent mapping by Myers (2002) led to the definition of low strain zones within the different tectonic panels of the ISB. The samples in this study were collected from one of these less deformed zones in the central tectonic domain, with the aim of minimizing geochemical effects of strain-controlled fluid percolation during tectono-metamorphism.

In contrast to “mobile” elements such as Rb, K, Na, Sr, Ba, Ca, Fe, P and Pb, which show variations in the Isua metavolcanic rocks (e.g., Frei et al., 2002; Polat et al., 2002a), a number of studies have found that in some Archean volcanic rocks the effects of alteration on REEs, HFSEs, Al, Cr and Ni are minor. Polat et al. (2002a) have assessed the effect of alteration on these elements in the metavolcanic rocks from the central tectonic domain. Based on an number of alteration criteria [noncoherent REE patterns characterized by variably large negative to positive Ce anomalies ( $Ce/Ce^* < 0.9$  and  $> 1.1$ ), high ( $> 6$  wt%) values of LOI (loss on ignition), significant carbonization and silicification ( $> 2\%$ )], Polat et al. (2002a) screened their sample set and considered only the least altered samples for their petrogenetic interpretation. A subset of this sample set of Polat et al. (2002a), in the following referred to as “least altered,” form the basis for the main isotopic-petrogenetic inferences from this study. According to Polat et al. (2002a), Th, REE, Ti, Zr and Nb in the least altered samples were immobile, as could be demonstrated by (1) systematic correlation between Zr and selected elements, (2) a lack of correlation of Th-Nb-La interelement relations with LOI, (3) a lack of correlation between intensity of deformation and the abundances of these elements, and (4) consistent and coherent primitive-mantle normalized trace element patterns.

### 3. SAMPLES AND ANALYTICAL TECHNIQUES

A set of samples from the boninite-like metabasaltic association from the central tectonic domain in the northeast sector of the ISB

(same powders as used by Polat et al., 2002a) was analyzed for Re-Os, Sm-Nd, and Pb isotopes. GPS readings of some of the “least altered” samples are listed in the Appendix and their locations plotted in Figure 1. All other samples from the northeast part of the ISB, from which coordinates are lacking, were collected within the same central tectonic domain.

Powder samples used for Re-Os isotopic analyses were attacked with inversed (14N HNO<sub>3</sub>:10N HCl = 3:1) aqua regia in Carius tubes at 230°C for 1 week. Os was distilled from inversed aqua regia directly into 8N HBr (Nägler and Frei, 1997) and purified according to the method of Roy-Barman and Allègre (1994). Samples were loaded in 1.5 μl 8N HBr onto high purity Pt filaments and 0.5 μl of a saturated Ba(OH)<sub>2</sub> solution was added as an ionization activator. Os isotopic analyses were performed on the VG Sector 54 solid-source negative thermal ionization mass spectrometer (N-TIMS) at the University of Copenhagen using single multiplier jump modes. Repeated analyses of 1 ng loads of the University of Maryland Johnson Matthey reference solution yielded an external reproducibility of ± 0.07% (2σ) of the ratio <sup>187</sup>Os/<sup>188</sup>Os = 0.11377 using <sup>189</sup>Os/<sup>188</sup>Os 0.121978 for in-run fractionation corrections.

Re was purified using the liquid extraction method by Cohen and Waters (1996) and the concentrations were measured on the quadrupole ICP-MS of the Geological Survey of Denmark and Greenland (GEUS), using Ir-doped sample solutions for controlling mass fractionation of Re by monitoring the <sup>190</sup>Ir/<sup>191</sup>Ir ratio. Procedural Re blanks remained below 15 pg (10 ± 5 pg, with natural composition) in the time during which the samples for this study were processed. Os procedure blanks were smaller than 15 pg (10 ± 5 pg, with <sup>187</sup>Os/<sup>188</sup>Os = 0.13 ± 0.02) at all times. Respective blank corrections for Re and Os were performed for each of the samples.

Dissolution of the powder samples used for Sm-Nd and Pb isotope analyses was achieved in two successive, but identical steps, which consisted of a strong 8N HBr attack (shown to effectively dissolve accessory phosphates (e.g., Frei et al., 1997; Schaller et al., 1997), followed by a concentrated HF-14N HNO<sub>3</sub> mix and finally by strong 9N HCl. Independent dissolutions were performed for REE and Pb analyses. A mixed <sup>150</sup>Nd/<sup>149</sup>Sm spike was added to the REE aliquot beforehand. Chemical separation of Sm and Nd was carried out on conventional cation exchange columns, followed by a separation using HDEHP-coated beads (BIO-RAD) charged in 6 mL quartz glass columns. Sm-Nd isotope analyses were carried out on a VG Sector 54-IT TIMS. Nd ratios were normalized to <sup>146</sup>Nd/<sup>144</sup>Nd = 0.7219. The mean value for our internal JM Nd standard (referenced against La Jolla) during the period of measurement was 0.511115 for <sup>145</sup>Nd/<sup>144</sup>Nd, with a 2σ external reproducibility of ± 0.000011 (five measurements). Procedural blanks run during the period of these analyses show insignificant blank levels of ~5 pg Sm and ~12 pg Nd. Precisions for concentration analysis are approximately 0.5% for Sm and Nd.

Sample powders used for Pb isotopes were gently leached in 2N HCl for 10 min. The leachates were pipetted off and processed separately. The residues were subsequently attacked and dissolved by the same sequential dissolution procedure described above. Pb was separated from the leachates and the residues. A conventional HCl-HBr elution recipe was used for both the separation over 0.5 mL glass columns charged with AG-1 x8 anion resin, and the final purification of the Pb concentrates over 300 μl Teflon columns. Procedural blanks for Pb remained below 87 pg, an amount which insignificantly affects the isotopic data of the samples analyzed herein. Fractionation for Pb was controlled by repeated analysis of the NBS 981 standard and amounted to 0.103 ± 0.007%/a.m.u. (2σ; n = 5) relative to the values proposed by Todt et al. (1993).

## 4. RESULTS

### 4.1. Sm-Nd Isotopes

Data from “least altered” boninite-like metabasalts from the central tectonic domain in the northeast sector of the ISB (Table 1) are plotted in a Sm-Nd isochron diagram in Figure 2. Data points plot along a correlation line with a slope corresponding to an age of 3.69 ± 0.18 Gy (MSWD = 3.5) which

Table 1. Whole rock Sm-Nd isotopic data of basalts and ultramafic rocks from the ISB.

| Sample*  | Rock                         | Degree of alteration | Unit <sup>#</sup> | Part of ISB | Sm (ppm) | Nd (ppm) | <sup>147</sup> Sm/ <sup>144</sup> Nd <sup>a</sup> | <sup>143</sup> Nd/ <sup>144</sup> Nd | ±2SE (abs.) | T <sub>CHUR</sub> <sup>§</sup> (Ga) | εNd(T) (T-0) | age T (Ma) | εNd(T) <sup>b</sup> | <sup>143</sup> Nd/ <sup>144</sup> Nd (initial; age T) | Reference                        |
|----------|------------------------------|----------------------|-------------------|-------------|----------|----------|---------------------------------------------------|--------------------------------------|-------------|-------------------------------------|--------------|------------|---------------------|-------------------------------------------------------|----------------------------------|
| 175553   | boninite-like metabasalt     | least altered        | GS                | W           | 0.71     | 2.57     | 0.167                                             | 0.512039                             | 0.000023    | 3.05                                | -11.7        | 3710       | 2.6                 | 0.507938                                              | this study                       |
| 175556   | boninite-like metabasalt     | least altered        | GS                | W           | 0.67     | 1.93     | 0.211                                             | 0.513119                             | 0.000034    | n.g.m.                              | 9.4          | 3710       | 2.7                 | 0.507943                                              | this study                       |
| 175557   | boninite-like metabasalt     | least altered        | GS                | W           | 0.77     | 2.73     | 0.172                                             | 0.512168                             | 0.000021    | 2.87                                | -9.2         | 3710       | 2.7                 | 0.507947                                              | this study                       |
| 175558   | boninite-like metabasalt     | least altered        | GS                | W           | 0.56     | 1.65     | 0.206                                             | 0.512993                             | 0.000039    | n.g.m.                              | 6.9          | 3710       | 2.7                 | 0.507945                                              | this study                       |
| 175561   | boninite-like metabasalt     | least altered        | GS                | W           | 0.86     | 2.21     | 0.236                                             | 0.513712                             | 0.000028    | 4.14                                | 21.0         | 3710       | 2.2                 | 0.507920                                              | this study                       |
| 810392   | boninite-like metabasalt     | least altered        | GS                | W           | 0.73     | 2.63     | 0.168                                             | 0.512045                             | 0.000007    | 3.11                                | -11.6        | 3710       | 2.3                 | 0.507922                                              | Blichert-Toft et al. (1999)      |
| 810071   | arc-like/picritic metabasalt | least altered        | Amph              | W           | 2.47     | 8.97     | 0.166                                             | 0.512028                             | 0.000009    | 3.06                                | -11.9        | 3810       | 3.0                 | 0.507827                                              | Blichert-Toft et al. (1999)      |
| 810155   | arc-like/picritic metabasalt | least altered        | Amph              | W           | 2.73     | 9.64     | 0.171                                             | 0.512176                             | 0.000007    | 2.77                                | -9.0         | 3810       | 3.5                 | 0.507851                                              | Blichert-Toft et al. (1999)      |
| 810425   | arc-like/picritic metabasalt | least altered        | Amph              | W           | 3.06     | 10.72    | 0.173                                             | 0.512129                             | 0.000015    | 3.18                                | -9.9         | 3810       | 2.0                 | 0.507776                                              | Blichert-Toft et al. (1999)      |
| 94-27    | arc-like/picritic metabasalt | least altered        | Amph              | W           | 0.94     | 3.20     | 0.178                                             | 0.512297                             | 0.000017    | 2.75                                | -6.7         | 3810       | 2.6                 | 0.507809                                              | Blichert-Toft et al. (1999)      |
| 94-66 C  | arc-like/picritic metabasalt | least altered        | Amph              | W           | 2.03     | 6.71     | 0.183                                             | 0.512470                             | 0.000007    | 1.91                                | -3.3         | 3810       | 3.3                 | 0.507844                                              | Frei et al. (2002)               |
| 94-66 D  | arc-like/picritic metabasalt | least altered        | Amph              | W           | 2.58     | 8.38     | 0.186                                             | 0.512445                             | 0.000006    | 2.76                                | -3.8         | 3810       | 1.5                 | 0.507750                                              | Frei et al. (2002)               |
| 94-66 E  | arc-like/picritic metabasalt | least altered        | Amph              | W           | 2.44     | 7.60     | 0.195                                             | 0.512653                             | 0.000007    | n.g.m.                              | 0.3          | 3810       | 1.4                 | 0.507745                                              | Frei et al. (2002)               |
| 94-66 F  | arc-like/picritic metabasalt | least altered        | Amph              | W           | 2.03     | 6.96     | 0.177                                             | 0.512294                             | 0.000015    | 2.59                                | -6.7         | 3810       | 3.2                 | 0.507839                                              | Frei et al. (2002)               |
| 810112   | arc-like/picritic metabasalt | variably latered     | Amph              | W           | 1.42     | 4.05     | 0.212                                             | 0.512963                             | 0.000011    | 3.16                                | 6.3          | 3810       | -1.3                | 0.507607                                              | Blichert-Toft et al. (1999)      |
| 810166   | boninite-like metabasalt     | variably latered     | GS                | W           | 0.36     | 1.02     | 0.215                                             | 0.513304                             | 0.000013    | n.g.m.                              | 13.0         | 3710       | 4.2                 | 0.508021                                              | Blichert-Toft et al. (1999)      |
| 810166 r | boninite-like metabasalt     | variably latered     | GS                | W           | 0.37     | 1.04     | 0.216                                             | 0.513373                             | 0.000018    | n.g.m.                              | 14.3         | 3710       | 4.9                 | 0.508057                                              | Blichert-Toft et al. (1999)      |
| 810423   | arc-like/picritic metabasalt | variably latered     | Amph              | W           | 2.71     | 7.05     | 0.233                                             | 0.513361                             | 0.000019    | 3.04                                | 14.1         | 3810       | -3.7                | 0.507490                                              | Blichert-Toft et al. (1999)      |
| 810423 r | arc-like/picritic metabasalt | variably latered     | Amph              | W           | 2.86     | 7.33     | 0.236                                             | 0.513435                             | 0.000011    | 3.09                                | 15.5         | 3810       | -3.7                | 0.507486                                              | Blichert-Toft et al. (1999)      |
| 930069   | boninite-like metabasalt     | variably latered     | GS                | W           | 0.44     | 1.13     | 0.235                                             | 0.513929                             | 0.000007    | n.g.m.                              | 25.2         | 3710       | 6.9                 | 0.508160                                              | this study                       |
| 930070   | boninite-like metabasalt     | variably latered     | GS                | W           | 0.50     | 1.30     | 0.233                                             | 0.513798                             | 0.000009    | n.g.m.                              | 22.6         | 3710       | 5.2                 | 0.508070                                              | this study                       |
| 94-66 A  | arc-like/picritic metabasalt | variably latered     | Amph              | W           | 2.05     | 7.51     | 0.165                                             | 0.512102                             | 0.000007    | 2.54                                | -10.5        | 3810       | 5.4                 | 0.507947                                              | Frei et al. (2002)               |
| 94-66 B  | arc-like/picritic metabasalt | variably latered     | Amph              | W           | 2.34     | 7.75     | 0.182                                             | 0.512412                             | 0.000007    | 2.38                                | -4.4         | 3810       | 2.7                 | 0.507813                                              | Frei et al. (2002)               |
| 460000   | ultramafic rock              | variably latered     | Amph              | W           | 0.07     | 0.22     | 0.200                                             | 0.512870                             | 0.000012    | n.g.m.                              | 4.5          | 3810       | 2.9                 | 0.507821                                              | Frei and Kastbjerg Jensen (2003) |
| 460015   | ultramafic rock              | variably latered     | Amph              | W           | 0.50     | 1.87     | 0.163                                             | 0.512390                             | 0.000007    | 1.11                                | -4.8         | 3810       | 12.1                | 0.508288                                              | Frei and Kastbjerg Jensen (2003) |
| 460092   | ultramafic rock              | least altered        | Amph              | W           | 0.15     | 0.38     | 0.234                                             | 0.513651                             | 0.000008    | 4.11                                | 19.8         | 3810       | 1.5                 | 0.507749                                              | Frei and Kastbjerg Jensen (2003) |
| 930043   | ultramafic rock              | least altered        | Amph              | W           | 0.35     | 0.89     | 0.237                                             | 0.513737                             | 0.000007    | 4.15                                | 21.4         | 3810       | 1.8                 | 0.507766                                              | Frei and Kastbjerg Jensen (2003) |
| BKJ 001  | ultramafic rock              | variably latered     | GS                | W           | 0.38     | 1.15     | 0.199                                             | 0.512884                             | 0.000007    | n.g.m.                              | 4.8          | 3710       | 3.9                 | 0.508007                                              | Frei and Kastbjerg Jensen (2003) |
| BKJ 002  | ultramafic rock              | variably latered     | GS                | W           | 0.37     | 1.30     | 0.171                                             | 0.512339                             | 0.000004    | 1.74                                | -5.8         | 3710       | 6.7                 | 0.508150                                              | Frei and Kastbjerg Jensen (2003) |
| BKJ 005  | ultramafic rock              | variably latered     | Amph              | W           | 0.07     | 0.20     | 0.199                                             | 0.513338                             | 0.000008    | n.g.m.                              | 13.7         | 3810       | 12.4                | 0.508307                                              | Frei and Kastbjerg Jensen (2003) |
| BKJ 006  | ultramafic rock              | variably latered     | Amph              | W           | 3.23     | 16.92    | 0.116                                             | 0.511130                             | 0.000004    | 2.81                                | -29.4        | 3810       | 10.6                | 0.508215                                              | Frei and Kastbjerg Jensen (2003) |
| BKJ 007  | ultramafic rock              | variably latered     | Amph              | W           | 6.49     | 33.79    | 0.116                                             | 0.510847                             | 0.000004    | 3.36                                | -34.9        | 3810       | 4.8                 | 0.507920                                              | Frei and Kastbjerg Jensen (2003) |
| BKJ 008  | ultramafic rock              | variably latered     | GS                | W           | 0.22     | 0.90     | 0.146                                             | 0.511699                             | 0.000005    | 2.82                                | -18.3        | 3710       | 5.9                 | 0.508108                                              | Frei and Kastbjerg Jensen (2003) |
| BKJ 009  | ultramafic rock              | variably latered     | Amph              | W           | 0.49     | 1.91     | 0.156                                             | 0.511900                             | 0.000004    | 2.75                                | -14.4        | 3810       | 5.7                 | 0.507964                                              | Frei and Kastbjerg Jensen (2003) |
| BKJ 010  | ultramafic rock              | variably latered     | Amph              | W           | 0.11     | 0.24     | 0.269                                             | 0.515067                             | 0.000011    | n.g.m.                              | 47.4         | 3810       | 11.9                | 0.508277                                              | Frei and Kastbjerg Jensen (2003) |
| BKJ 011  | ultramafic rock              | variably latered     | Amph              | W           | 0.16     | 0.33     | 0.294                                             | 0.515372                             | 0.000008    | 4.25                                | 53.3         | 3810       | 5.7                 | 0.507962                                              | Frei and Kastbjerg Jensen (2003) |

Table 1. (Continued)

| Sample*   | Rock                     | Degree of alteration       | Unit <sup>#</sup> | Part of ISB | Sm (ppm) | Nd (ppm) | <sup>147</sup> Sm/ <sup>144</sup> Nd <sup>‡</sup> | <sup>143</sup> Nd/ <sup>144</sup> Nd | ±2SE (abs.) | T <sub>CHUR</sub> <sup>§</sup> (Ga) | εNd(T) (T-0) | age T (Ma) | εNd(T) <sup>b</sup> | <sup>143</sup> Nd/ <sup>144</sup> Nd (initial; age T) | Reference                        |
|-----------|--------------------------|----------------------------|-------------------|-------------|----------|----------|---------------------------------------------------|--------------------------------------|-------------|-------------------------------------|--------------|------------|---------------------|-------------------------------------------------------|----------------------------------|
| BKJ 013   | ultramafic rock          | variably latered           | GS                | W           | 0.02     | 0.07     | 0.199                                             | 0.513062                             | 0.000027    | n.g.m.                              | 8.3          | 3810       | 7.4                 | 0.508050                                              | Frei and Kastbjerg Jensen (2003) |
| BKJ 014   | ultramafic rock          | least altered              | Amph              | W           | 0.16     | 0.28     | 0.344                                             | 0.516481                             | 0.000014    | 3.94                                | 75.0         | 3810       | 2.5                 | 0.507804                                              | Frei and Kastbjerg Jensen (2003) |
| BKJ 014   | ultramafic rock          | least altered              | Amph              | W           | 0.16     | 0.29     | 0.341                                             | 0.516390                             | 0.000011    | 3.92                                | 73.2         | 3810       | 2.1                 | 0.507784                                              | this study                       |
| BKJ 015   | ultramafic rock          | variably latered           | GS                | W           | 0.04     | 0.11     | 0.211                                             | 0.513540                             | 0.000012    | n.g.m.                              | 17.6         | 3710       | 10.8                | 0.508356                                              | Frei and Kastbjerg Jensen (2003) |
| BKJ 015 r | ultramafic rock          | variably altered           | GS                | W           | 0.04     | 0.11     | 0.207                                             | 0.513213                             | 0.000004    | n.g.m.                              | 11.2         | 3710       | 6.5                 | 0.508139                                              | Frei and Kastbjerg Jensen (2003) |
| BKJ 019   | ultramafic rock          | variably latered           | GS                | W           | 0.08     | 0.24     | 0.203                                             | 0.513107                             | 0.000010    | n.g.m.                              | 9.1          | 3710       | 6.3                 | 0.508124                                              | Frei and Kastbjerg Jensen (2003) |
| 242727H   | ultramafic rock          | variably altered           | GS                | NE          | 0.20     | 0.46     | 0.268                                             | 0.512490                             | 0.000019    | n.g.m.                              | -2.9         | 3710       | -37.3               | 0.505914                                              | this study                       |
| 242670    | boninite-like metabasalt | least altered              | GS                | NE          | 0.63     | 2.30     | 0.172                                             | 0.512128                             | 0.000010    | 3.11                                | -9.9         | 3710       | 1.9                 | 0.507906                                              | this study                       |
| 242671    | boninite-like metabasalt | least altered              | GS                | NE          | 0.76     | 2.66     | 0.173                                             | 0.512225                             | 0.000007    | 2.65                                | -8.0         | 3710       | 3.3                 | 0.507974                                              | this study                       |
| 242718    | boninite-like metabasalt | least altered              | GS                | NE          | 0.42     | 1.20     | 0.213                                             | 0.513133                             | 0.000006    | n.g.m.                              | 9.7          | 3710       | 2.0                 | 0.507911                                              | this study                       |
| 242717A   | boninite-like metabasalt | least altered              | GS                | NE          | 0.39     | 1.08     | 0.221                                             | 0.513305                             | 0.000003    | 4.14                                | 13.0         | 3710       | 1.4                 | 0.507878                                              | this study                       |
| 242719C   | boninite-like metabasalt | least altered              | GS                | NE          | 0.38     | 0.98     | 0.233                                             | 0.513600                             | 0.000007    | 3.99                                | 18.8         | 3710       | 1.3                 | 0.507875                                              | this study                       |
| 242725    | boninite-like metabasalt | least altered              | GS                | NE          | 0.36     | 0.94     | 0.230                                             | 0.513635                             | 0.000005    | 4.49                                | 19.5         | 3710       | 3.5                 | 0.507982                                              | this study                       |
| 242733    | boninite-like metabasalt | least altered              | GS                | NE          | 0.68     | 1.73     | 0.239                                             | 0.513852                             | 0.000005    | 4.36                                | 23.7         | 3710       | 3.6                 | 0.507990                                              | this study                       |
| 242742    | boninite-like metabasalt | least altered              | GS                | NE          | 0.52     | 1.63     | 0.192                                             | 0.512577                             | 0.000005    | 2.10                                | -1.2         | 3710       | 0.9                 | 0.507855                                              | this study                       |
| 242744    | boninite-like metabasalt | least altered              | GS                | NE          | 0.74     | 2.14     | 0.210                                             | 0.512986                             | 0.000010    | 4.05                                | 6.8          | 3710       | 0.6                 | 0.507837                                              | this study                       |
| 242790A   | boninite-like metabasalt | least altered              | GS                | NE          | 0.61     | 1.79     | 0.208                                             | 0.513062                             | 0.000006    | n.g.m.                              | 8.3          | 3710       | 2.9                 | 0.507955                                              | this study                       |
| 462901    | boninite-like metabasalt | least altered              | GS                | NE          | 0.39     | 1.06     | 0.225                                             | 0.513386                             | 0.000006    | 3.96                                | 14.6         | 3710       | 1.0                 | 0.507855                                              | this study                       |
| 462902    | boninite-like metabasalt | least altered              | GS                | NE          | 0.41     | 1.18     | 0.210                                             | 0.513113                             | 0.000005    | n.g.m.                              | 9.3          | 3710       | 2.8                 | 0.507951                                              | this study                       |
| 462903    | boninite-like metabasalt | least altered              | GS                | NE          | 0.60     | 1.88     | 0.194                                             | 0.512683                             | 0.000016    | n.g.m.                              | 0.9          | 3710       | 2.2                 | 0.507921                                              | this study                       |
| 462904    | boninite-like metabasalt | least altered              | GS                | NE          | 0.62     | 1.86     | 0.202                                             | 0.512824                             | 0.000006    | n.g.m.                              | 3.6          | 3710       | 1.2                 | 0.507866                                              | this study                       |
| 462945    | boninite-like metabasalt | least altered              | GS                | NE          | 0.54     | 1.55     | 0.211                                             | 0.513138                             | 0.000007    | n.g.m.                              | 9.7          | 3710       | 3.0                 | 0.507957                                              | this study                       |
| 462946    | boninite-like metabasalt | least altered              | GS                | NE          | 0.66     | 1.89     | 0.211                                             | 0.513073                             | 0.000005    | n.g.m.                              | 8.5          | 3710       | 1.7                 | 0.507896                                              | this study                       |
| 462947    | boninite-like metabasalt | least altered              | GS                | NE          | 0.61     | 1.80     | 0.204                                             | 0.512943                             | 0.000007    | n.g.m.                              | 6.0          | 3710       | 2.3                 | 0.507922                                              | this study                       |
| 462948    | boninite-like metabasalt | least altered              | GS                | NE          | 0.79     | 2.31     | 0.207                                             | 0.512980                             | 0.000007    | n.g.m.                              | 6.7          | 3710       | 1.9                 | 0.507902                                              | this study                       |
| 462949    | boninite-like metabasalt | least altered              | GS                | NE          | 0.61     | 1.79     | 0.208                                             | 0.512958                             | 0.000005    | 4.31                                | 6.2          | 3710       | 0.9                 | 0.507852                                              | this study                       |
| 462965    | boninite-like metabasalt | least altered              | GS                | NE          | 0.33     | 0.81     | 0.243                                             | 0.513796                             | 0.000005    | 3.79                                | 22.6         | 3710       | 0.5                 | 0.507831                                              | this study                       |
| 462968    | boninite-like metabasalt | least altered              | GS                | NE          | 0.52     | 1.51     | 0.208                                             | 0.513002                             | 0.000008    | n.g.m.                              | 7.1          | 3710       | 1.7                 | 0.507893                                              | this study                       |
| 462966    | boninite-like metabasalt | least altered <sup>†</sup> | GS                | NE          | 0.32     | 0.82     | 0.235                                             | 0.513078                             | 0.000006    | 1.75                                | 8.6          | 3710       | -9.8                | 0.507311                                              | this study                       |
| 462906    | boninite-like metabasalt | least altered <sup>†</sup> | GS                | NE          | 0.43     | 0.83     | 0.315                                             | 0.513073                             | 0.000024    | 0.56                                | 8.5          | 3710       | -48.6               | 0.505338                                              | this study                       |
| 242729    | boninite-like metabasalt | least altered <sup>†</sup> | GS                | NE          | 0.14     | 0.56     | 0.150                                             | 0.513178                             | 0.000012    | n.g.m.                              | 10.5         | 3710       | 33.4                | 0.509504                                              | this study                       |
| 243689    | boninite-like metabasalt | least altered <sup>†</sup> | GS                | NE          | 0.74     | 2.12     | 0.209                                             | 0.512618                             | 0.000007    | n.g.m.                              | -0.4         | 3710       | -6.5                | 0.507475                                              | this study                       |
| 242737    | boninite-like basalt     | variably altered           | GS                | NE          | 0.19     | 0.45     | 0.259                                             | 0.514061                             | 0.000011    | 3.47                                | 27.8         | 3710       | -2.0                | 0.507706                                              | this study                       |
| 242743    | boninite-like basalt     | variably altered           | GS                | NE          | 0.31     | 0.76     | 0.247                                             | 0.513245                             | 0.000009    | 1.83                                | 11.8         | 3710       | -12.4               | 0.507178                                              | this study                       |
| 242673B   | boninite-like basalt     | variably altered           | GS                | NE          | 0.40     | 1.06     | 0.228                                             | 0.513470                             | 0.000006    | 4.06                                | 16.2         | 3710       | 1.4                 | 0.507880                                              | this study                       |
| 462927    | boninite-like basalt     | variably altered           | GS                | NE          | 0.41     | 0.94     | 0.193                                             | 0.512567                             | 0.000009    | 2.55                                | -1.4         | 3710       | 0.6                 | 0.507840                                              | this study                       |

\* r = repeat analysis.

<sup>†</sup> Termed "least altered" by Polat et al. (2002), but showing disturbed Sm-Nd isotope systematics.<sup>#</sup> GS = Garbenschiefer Unit; Amph = Amphibolite Unit; whr = whole roc.<sup>§</sup> The error on this ratio is ±0.2%.<sup>§</sup> n.g.m. = not geologically meaningful.<sup>b</sup> Values calculated using <sup>143</sup>Nd/<sup>144</sup>Nd = 0.512638 and <sup>147</sup>Sm/<sup>144</sup>Nd = 0.1966 for the present-day chondritic reservoir. Decay constant λ for <sup>147</sup>Sm = 6.54 × 10<sup>-12</sup>a<sup>-1</sup>.

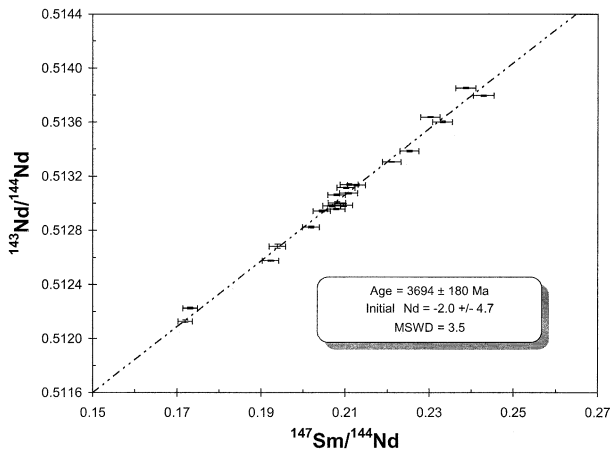


Fig. 2. Sm-Nd isotope diagram with data from “least altered” boninite-like metabasalts from the northeast central tectonic domain of the ISB. Data define a correlation line with a slope corresponding to an age of  $3.69 \pm 0.18$  Gy (MSWD = 3.5), which is in accordance with (more precise) indirect age constraints for their formation with U-Pb zircon geochronological results (3.69–3.71 Gy) obtained from metagranitoids emplaced into the metavolcanic sequences (Nutman et al., 1997).

defines an initial, but highly uncertain  $\epsilon\text{Nd}$  value of  $\sim +2 \pm 4.7$ . The age corresponds well with the proposed formation age of between 3.69–3.71 Gy for this suite, which is based on U-Pb zircon ages of metagranitoids emplaced within the metavolcanic sequences of the ISB (Nutman et al., 1997). Data from these boninite-like metabasalts, together with data of ultramafic rocks and least altered metabasalts (Blichert-Toft et al., 1999; Frei et al., 2002; Frei and Kastbjerg Jensen, 2003) from the outer tectonic domain in the W part of the ISB (Table 1), are additionally plotted in an  $\epsilon\text{Nd}$  [T = 3.71 Gy for central tectonic domain metabasalts; T = 3.81 Gy for outer tectonic domain metabasalts] vs. Nd concentration diagram (Fig. 3). Boninite-like metabasalts have lower Nd concentrations than the metabasalts from the outer tectonic domain, but they cannot be distinguished by their average initial Nd isotopic compositions. “Least altered” boninite-like metabasalts from the northeast part of the ISB are characterized by an average  $\epsilon\text{Nd}$  [T = 3.71 Ga] value of  $+2.2 \pm 0.9$  ( $n = 18$ ;  $1\sigma$ ). This value is indistinguishable from the average  $\epsilon\text{Nd}$  [T = 3.71 Ga] value of  $+2.9 \pm 1.6$  ( $n = 8$ ,  $1\sigma$ ) of a number of pillow cores from the boninite-like metabasaltic suite in the northeast central tectonic domain (recalculated after values in table 4 of Polat et al., 2002b) and it agrees with the average  $\epsilon\text{Nd}$  [T = 3.71 Ga] value of  $+2.5 \pm 0.2$  ( $n = 6$ ;  $1\sigma$ ) from boninite-like metabasalts from the W part of the ISB (this study, Table 1). Furthermore it is also compatible with the average  $\epsilon\text{Nd}$  [T = 3.81 Ga] value of  $+2.6 \pm 0.8$  ( $n = 8$ ;  $1\sigma$ ) for the older, arc-like, picritic metabasalts from the W part (data in Blichert-Toft et al., 1999, and Frei et al., 2002, listed in Table 1 for completion). The positive initial  $\epsilon\text{Nd}$  values indicate a depleted nature of their mantle source. The comparatively broad variation in  $\epsilon\text{Nd}$  values of ultramafic rocks with generally low Nd concentrations most likely reflects the effect of alteration of these rocks (Fig. 3), i.e., the increased tendency of open system behavior of the Sm-Nd isotopic system on the scale of whole rocks. Boninite-like metabasalts that have been classified as “variably altered” by

Polat et al. (2002a) show a wide range of geologically unreasonable  $\epsilon\text{Nd}$  [T = 3.71 Ga] values ranging from  $-37.3$  to  $+6.5$  (Table 1), which confirm that these samples were disturbed in their REE systematics. However, we also found four samples (listed at the end of Table 1) classified as “least altered” by Polat et al. (2002a) that show disturbed Sm-Nd systematics ( $\epsilon\text{Nd}$  [T = 3.71 Ga] values between  $-48.6$  and  $+33.4$ ). This demonstrates the sensitivity of the Sm-Nd isotopic tracer system beyond the sensitivity of trace elements to disturbances in rocks with low REE concentrations by postformational metamorphic-metasomatic processes. It also reinforces the conclusion that the majority of the boninite-like metabasalts that were labeled “least altered” by Polat et al. (2002a) do not show evidence of disturbance to the Sm-Nd isotopic system.

## 4.2. Re-Os Isotopes

Re-Os isotopic data of 11 boninite-like meta-basalts from the central tectonic domain in the northeast part of the ISB, categorized as “least altered” by Polat et al. (2002a), are listed in Table 2. The samples are characterized by very high Os concentrations, varying between 1.7 and 3.7 ppb, and by fairly normal Re concentrations of the order of several hundred ppt. The Os concentrations are higher than those typically characterizing komatiitic basalts (0.05–0.21 ppb; Puchtel and Humayun, 2001a,b) and komatiites (0.8–1.8 ppb; Puchtel and Humayun, 2000) and are similar to the value of  $\sim 3.3$  ppb estimated for the primitive upper mantle (Puchtel and Humayun, 2000; Meisel et al., 2001). Re-Os isotopic data are plotted in an isochron diagram in Figure 4. Omitting from the linear regression analysis three data points (samples 462901, 462902 and 242790A) that show disturbed Re-Os isotope systematics, all other samples plot along an isochron defining an age of  $3762 \pm 90$  My (MSWD = 1.4). This age is in agreement with the

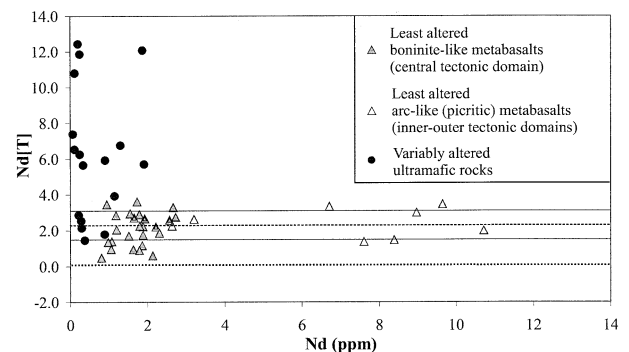


Fig. 3. Nd (ppm) versus  $\epsilon\text{Nd}$  (T = 3.71 Ga for boninite-like metabasalts; T = 3.81 Ga for arc-like, picritic metabasalts and ultramafic rocks) diagram of metavolcanic rocks from the ISB. Boninite-like metabasalts from the northeast central tectonic domain have lower Nd concentrations than the picritic suite, but their average  $\epsilon\text{Nd}$  value of  $+2.2 \pm 0.9$  (average marked by the dashed line, error-band outlined by thin solid lines) does not distinguish them from the older, arc-like, picritic suite. These data indicate a significant depletion of their mantle sources, probably in the Hadean. Ultramafic rocks (data from Frei and Kastbjerg Jensen, 2003; two data point with very high Nd concentrations outside plot limits) that are tectonically intercalated with both metavolcanic suites in the W part of the ISB show a wide scatter in  $\epsilon\text{Nd}$  values and record significant postformational disturbance of the Sm-Nd system in these rocks, enhanced by their low overall REE concentrations.

Table 2. Whole rock Re-Os isotopic data of least altered boninite-like metabasalts from the NE part of the ISB.<sup>a</sup>

| Sample  | Alteration                           | Re (ppt) | Os (ppt) | <sup>187</sup> Os/ <sup>188</sup> Os | ±2 SE   | <sup>187</sup> Re/ <sup>188</sup> Os |
|---------|--------------------------------------|----------|----------|--------------------------------------|---------|--------------------------------------|
| 462968  | least altered                        | 505      | 1907     | 0.18646                              | 0.00053 | 1.25                                 |
| 242670  | least altered                        | 687      | 3229     | 0.17032                              | 0.00018 | 1.01                                 |
| 462904  | least altered                        | 327      | 2380     | 0.14689                              | 0.00012 | 0.65                                 |
| 462945  | least altered                        | 458      | 3332     | 0.14753                              | 0.00028 | 0.65                                 |
| 462949  | least altered                        | 432      | 3138     | 0.14659                              | 0.00016 | 0.65                                 |
| 462965  | least altered                        | 957      | 2883     | 0.20566                              | 0.00028 | 1.57                                 |
| 462946  | least altered                        | 274      | 1664     | 0.15652                              | 0.00018 | 0.78                                 |
| 462948  | least altered                        | 408      | 3401     | 0.14171                              | 0.00019 | 0.57                                 |
|         | average                              | 506      | 2742     |                                      |         |                                      |
|         | ±2σ                                  | 440      | 1349     |                                      |         |                                      |
| 462901  | disturbed Re-Os isotopic systematics | 349      | 1948     | 0.14327                              | 0.00007 | 0.85                                 |
| 462902  | disturbed Re-Os isotopic systematics | 658      | 2138     | 0.17488                              | 0.00024 | 1.46                                 |
| 242790A | disturbed Re-Os isotopic systematics | 335      | 3667     | 0.13073                              | 0.00016 | 0.43                                 |

<sup>a</sup>  $\gamma$ Os is calculated using the parameters from Shirey and Walker (1998) and  $\lambda^{187}\text{Re} = 1.666 \times 10^{-11} \text{a}^{-1}$  (Smoliar et al., 1996). Uncertainties are ±2% or better for Re concentrations. The uncertainty in Os concentrations is better than ±0.2%, and within-run two standard errors (SE) are specified for the <sup>187</sup>Os. The maximum uncertainty of the  $\gamma$ Os [T = 3.71 Ga] values is ±0.5 units.

assumed extrusion age of ~3.71 Gy (Nutman et al., 1997). Calculated initial <sup>187</sup>Os/<sup>188</sup>Os isotopic values, based on a 3.71 Gy maximum extrusion age, vary between suprachondritic values of 0.1032–0.1067, with corresponding  $\gamma$ Os values ranging between +1.7 and +5.3 (average  $\gamma$ Os [T = 3.71 Ga] = +4.4 ± 1.2, n = 8; 2σ), respectively (Table 2). As with a few examples of “least altered” samples, which show disturbed Sm-Nd isotopic systematics, it appears that the Re-Os isotopic tracer system is sensitive to metamorphism/metasomatism beyond the trace elemental criteria used to discriminate “variably altered” from “least altered” by Polat et al. (2002a). This is consistent with the finding of Frei and Kastbjerg Jensen (2003) based on analyses of metabasalts and ultramafic rocks from the W part of the ISB. However, the majority of the “least altered”

samples used in this study show no signs of disturbance to the Re-Os isotopic system.

### 4.3. Pb Isotopes

Pb isotopic data of leachates and residues of “least altered” and “variably altered” boninite-like metabasalts are listed in Table 3 and plotted in uranogenic and uranogenic-thorogenic common Pb isotope diagrams in Figure 5. It is obvious that gentle leaching is capable of removing excessive scatter in the data (open symbols), both in uranogenic and uranogenic-thorogenic Pb isotope space. Furthermore, it can be seen that samples termed “least altered” (Table 3) show the least scatter of their residues; data points plot around a correlation line in the uranogenic diagram (Fig. 5a) with a slope corresponding to an age of 3510 ± 65 Ma (MSWD = 97). Respective leached fractions of these “least altered” samples (open squares) scatter around this reference line, but in uranogenic-thorogenic space (Fig. 5b) they are dominated by higher <sup>208</sup>Pb/<sup>204</sup>Pb ratios relative to <sup>206</sup>Pb/<sup>204</sup>Pb ratios of comparable residues. The samples with the most radiogenic Pb isotope ratios in uranogenic space (Fig. 5a) are also those with the highest <sup>208</sup>Pb/<sup>204</sup>Pb ratios of their leachates (Fig. 5b), implying that the Pb budget in these samples is dominated by a phase with higher Th/U than that of most of the bulk samples, from which its Pb is easily leachable. This is consistent with the findings of Frei et al. (2002) on metabasalts from the outer tectonic domain in the W part of the ISB, which linked elevated <sup>208</sup>Pb/<sup>204</sup>Pb relative to <sup>206</sup>Pb/<sup>204</sup>Pb ratios to the presence of allanite formed during Early/Late Archean metasomatic fluid percolation. The correlation line with a slope corresponding to an age of 3510 ± 65 Ma is interpreted to date Pb-loss during an Early Archean metamorphic event. This age is identical within error to the metamorphic overprinting at ca. 3560–3580 Ma proposed by Nutman et al. (2002) on the basis of U-Pb data of metamorphic overgrowths on zircons from intrusive tonalite sheets into the “Garbenschiefer” unit. The Pb isotopic data in general indicate disturbance of the U-Th-Pb system, possibly due to the generally high mobility of Pb under metamorphic conditions and/or during postformational metasomatic-hydrothermal alteration processes. Polat et al. (2002a,b) noticed excessive scatter of Pb

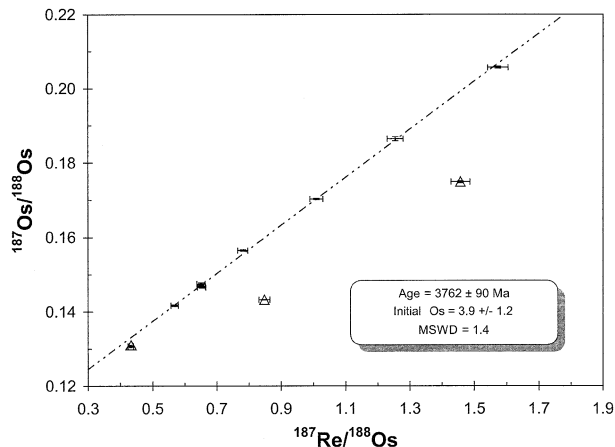


Fig. 4. Re-Os isochron diagram with data of boninite-like metabasalts from the northeast central tectonic domain of the ISB. With the exception of three samples, which show disturbed Re-Os isotopic systematics, eight samples define an isochron with an age of 3763 ± 90 My (MSWD = 1.4). This age, within error, is identical with the assumed extrusion age of ~3.71 Gy (Nutman et al., 1997) for this suite. The three “outliers” indicate that the Re-Os isotopic system is sensitive beyond the trace elemental criteria used for discriminating “variably altered” from “least altered” samples by Polat et al. (2002a). The initial <sup>187</sup>Os/<sup>188</sup>Os ratio of 0.1050 ± 0.0012 indicates a significantly suprachondritic component in the source of these basalts. See text for discussion.

Table 3. Whole rock Pb isotope data of boninite-like basalts from the NE part of the ISB.

| Sample           | Alteration <sup>§</sup> | Phase    | <sup>206</sup> Pb/<br><sup>204</sup> Pb | ±2σ <sup>†</sup> | <sup>207</sup> Pb/<br><sup>204</sup> Pb | ±2σ <sup>†</sup> | <sup>208</sup> Pb/<br><sup>204</sup> Pb | ±2σ <sup>†</sup> | r <sub>1</sub> ** | r <sub>2</sub> ** | U##<br>(ppm) | Th#<br>(ppm) | Pb#<br>(ppm) | <sup>206</sup> Pb/ <sup>204</sup> Pb*<br><i>in situ</i> corr. | <sup>207</sup> Pb/ <sup>204</sup> Pb*<br><i>in situ</i> corr. | <sup>208</sup> Pb/ <sup>204</sup> Pb*<br><i>in situ</i> corr. |  |  |
|------------------|-------------------------|----------|-----------------------------------------|------------------|-----------------------------------------|------------------|-----------------------------------------|------------------|-------------------|-------------------|--------------|--------------|--------------|---------------------------------------------------------------|---------------------------------------------------------------|---------------------------------------------------------------|--|--|
| <i>Leachates</i> |                         |          |                                         |                  |                                         |                  |                                         |                  |                   |                   |              |              |              |                                                               |                                                               |                                                               |  |  |
| 242670           | least altered           | leachate | 13.317                                  | 0.009            | 14.175                                  | 0.011            | 33.272                                  | 0.030            | 0.965             | 0.937             | —            | —            | —            | —                                                             | —                                                             | —                                                             |  |  |
| 242671B          | least altered           | leachate | 13.521                                  | 0.011            | 14.284                                  | 0.013            | 33.151                                  | 0.033            | 0.963             | 0.942             | —            | —            | —            | —                                                             | —                                                             | —                                                             |  |  |
| 242718           | least altered           | leachate | 13.039                                  | 0.010            | 14.017                                  | 0.012            | 33.099                                  | 0.031            | 0.963             | 0.929             | —            | —            | —            | —                                                             | —                                                             | —                                                             |  |  |
| 242725           | least altered           | leachate | 12.988                                  | 0.043            | 14.002                                  | 0.047            | 32.961                                  | 0.112            | 0.988             | 0.979             | —            | —            | —            | —                                                             | —                                                             | —                                                             |  |  |
| 242733           | least altered           | leachate | 14.427                                  | 0.021            | 14.380                                  | 0.022            | 34.546                                  | 0.055            | 0.975             | 0.968             | —            | —            | —            | —                                                             | —                                                             | —                                                             |  |  |
| 242742           | least altered           | leachate | 17.631                                  | 0.128            | 15.390                                  | 0.113            | 37.937                                  | 0.277            | 0.993             | 0.995             | —            | —            | —            | —                                                             | —                                                             | —                                                             |  |  |
| 242744           | least altered           | leachate | 16.422                                  | 0.022            | 14.863                                  | 0.021            | 36.605                                  | 0.054            | 0.974             | 0.951             | —            | —            | —            | —                                                             | —                                                             | —                                                             |  |  |
| 462901           | least altered           | leachate | 12.349                                  | 0.017            | 13.754                                  | 0.020            | 32.387                                  | 0.049            | 0.971             | 0.964             | —            | —            | —            | —                                                             | —                                                             | —                                                             |  |  |
| 462902           | least altered           | leachate | 12.159                                  | 0.006            | 13.679                                  | 0.008            | 32.104                                  | 0.023            | 0.967             | 0.939             | —            | —            | —            | —                                                             | —                                                             | —                                                             |  |  |
| 462903           | least altered           | leachate | 12.572                                  | 0.008            | 13.756                                  | 0.010            | 32.582                                  | 0.028            | 0.961             | 0.926             | —            | —            | —            | —                                                             | —                                                             | —                                                             |  |  |
| 462904           | least altered           | leachate | 12.709                                  | 0.010            | 13.801                                  | 0.012            | 32.509                                  | 0.033            | 0.952             | 0.922             | —            | —            | —            | —                                                             | —                                                             | —                                                             |  |  |
| 462945           | least altered           | leachate | 12.372                                  | 0.009            | 13.686                                  | 0.011            | 32.369                                  | 0.031            | 0.956             | 0.909             | —            | —            | —            | —                                                             | —                                                             | —                                                             |  |  |
| 462946           | least altered           | leachate | 14.937                                  | 0.033            | 14.172                                  | 0.033            | 35.925                                  | 0.084            | 0.979             | 0.975             | —            | —            | —            | —                                                             | —                                                             | —                                                             |  |  |
| 462947           | least altered           | leachate | 14.998                                  | 0.013            | 14.157                                  | 0.013            | 35.227                                  | 0.036            | 0.969             | 0.935             | —            | —            | —            | —                                                             | —                                                             | —                                                             |  |  |
| 462948           | least altered           | leachate | 13.514                                  | 0.018            | 13.864                                  | 0.020            | 33.959                                  | 0.050            | 0.978             | 0.966             | —            | —            | —            | —                                                             | —                                                             | —                                                             |  |  |
| 462949           | least altered           | leachate | 14.975                                  | 0.015            | 14.133                                  | 0.015            | 36.626                                  | 0.042            | 0.965             | 0.943             | —            | —            | —            | —                                                             | —                                                             | —                                                             |  |  |
| 462965           | least altered           | leachate | 12.964                                  | 0.013            | 13.927                                  | 0.015            | 32.999                                  | 0.041            | 0.944             | 0.880             | —            | —            | —            | —                                                             | —                                                             | —                                                             |  |  |
| 462966           | least altered           | leachate | failed                                  | —                | —                                       | —                | —                                       | —                | —                 | —                 | —            | —            | —            | —                                                             | —                                                             | —                                                             |  |  |
| 462967           | least altered           | leachate | 12.355                                  | 0.009            | 13.777                                  | 0.012            | 32.353                                  | 0.031            | 0.963             | 0.916             | —            | —            | —            | —                                                             | —                                                             | —                                                             |  |  |
| 242717a          | least altered           | leachate | failed                                  | —                | —                                       | —                | —                                       | —                | —                 | —                 | —            | —            | —            | —                                                             | —                                                             | —                                                             |  |  |
| 242719C          | least altered           | leachate | 12.307                                  | 0.007            | 13.771                                  | 0.009            | 32.254                                  | 0.026            | 0.947             | 0.915             | —            | —            | —            | —                                                             | —                                                             | —                                                             |  |  |
| 242790a          | least altered           | leachate | 11.789                                  | 0.034            | 13.439                                  | 0.040            | 31.621                                  | 0.095            | 0.985             | 0.973             | —            | —            | —            | —                                                             | —                                                             | —                                                             |  |  |
| 242729           | variably altered        | leachate | 12.545                                  | 0.006            | 13.834                                  | 0.008            | 32.480                                  | 0.024            | 0.967             | 0.938             | —            | —            | —            | —                                                             | —                                                             | —                                                             |  |  |
| 242737           | variably altered        | leachate | 15.588                                  | 0.013            | 14.896                                  | 0.014            | 35.336                                  | 0.035            | 0.967             | 0.939             | —            | —            | —            | —                                                             | —                                                             | —                                                             |  |  |
| 242743           | variably altered        | leachate | 15.413                                  | 0.054            | 14.696                                  | 0.053            | 35.567                                  | 0.128            | 0.989             | 0.987             | —            | —            | —            | —                                                             | —                                                             | —                                                             |  |  |
| 243689           | variably altered        | leachate | 13.164                                  | 0.013            | 14.183                                  | 0.016            | 32.318                                  | 0.043            | 0.939             | 0.832             | —            | —            | —            | —                                                             | —                                                             | —                                                             |  |  |
| 462906           | variably altered        | leachate | 12.392                                  | 0.007            | 13.808                                  | 0.009            | 32.299                                  | 0.025            | 0.954             | 0.933             | —            | —            | —            | —                                                             | —                                                             | —                                                             |  |  |
| 242673B          | variably altered        | leachate | 13.070                                  | 0.010            | 14.245                                  | 0.012            | 32.138                                  | 0.031            | 0.955             | 0.924             | —            | —            | —            | —                                                             | —                                                             | —                                                             |  |  |
| 242727H          | variably altered        | leachate | 13.275                                  | 0.021            | 14.106                                  | 0.024            | 33.253                                  | 0.057            | 0.974             | 0.971             | —            | —            | —            | —                                                             | —                                                             | —                                                             |  |  |
| <i>Residues</i>  |                         |          |                                         |                  |                                         |                  |                                         |                  |                   |                   |              |              |              |                                                               |                                                               |                                                               |  |  |
| 242670           | least altered           | residue  | 12.459                                  | 0.012            | 13.848                                  | 0.016            | 32.243                                  | 0.045            | 0.933             | 0.794             | 0.111        | 0.325        | 3.39         | 11.025                                                        | 13.406                                                        | 30.689                                                        |  |  |
| 242671B          | least altered           | residue  | 15.792                                  | 0.015            | 14.889                                  | 0.015            | 34.069                                  | 0.037            | 0.967             | 0.948             | 0.058        | 0.290        | 2.68         | 14.208                                                        | 14.401                                                        | 32.354                                                        |  |  |
| 242718           | least altered           | residue  | 12.678                                  | 0.014            | 13.879                                  | 0.016            | 32.421                                  | 0.040            | 0.971             | 0.953             | —            | 0.116        | 2.69         | 11.233                                                        | 13.434                                                        | 30.856                                                        |  |  |
| 242725           | least altered           | residue  | 12.475                                  | 0.015            | 13.868                                  | 0.018            | 32.308                                  | 0.044            | 0.966             | 0.939             | 0.002        | 0.046        | 1.80         | 11.038                                                        | 13.426                                                        | 30.751                                                        |  |  |
| 242733           | least altered           | residue  | 13.283                                  | 0.015            | 14.060                                  | 0.017            | 32.766                                  | 0.042            | 0.959             | 0.948             | 0.008        | 0.044        | 1.03         | 11.811                                                        | 13.607                                                        | 31.171                                                        |  |  |
| 242742           | least altered           | residue  | 20.276                                  | 0.015            | 16.163                                  | 0.014            | 36.403                                  | 0.034            | 0.941             | 0.930             | 0.011        | 0.221        | 1.09         | 18.498                                                        | 15.615                                                        | 34.477                                                        |  |  |
| 242744           | least altered           | residue  | 13.711                                  | 0.009            | 14.155                                  | 0.011            | 33.165                                  | 0.032            | 0.959             | 0.879             | 0.014        | 0.218        | 1.25         | 12.216                                                        | 13.695                                                        | 31.546                                                        |  |  |
| 462901           | least altered           | residue  | 12.369                                  | 0.008            | 13.781                                  | 0.011            | 32.131                                  | 0.028            | 0.961             | 0.930             | 0.003        | 0.078        | 3.10         | 10.941                                                        | 13.341                                                        | 30.584                                                        |  |  |
| 462902           | least altered           | residue  | 12.604                                  | 0.027            | 13.817                                  | 0.031            | 32.390                                  | 0.074            | 0.985             | 0.969             | —            | 0.098        | —            | —                                                             | —                                                             | —                                                             |  |  |
| 462903           | least altered           | residue  | 12.257                                  | 0.005            | 13.708                                  | 0.008            | 32.063                                  | 0.023            | 0.967             | 0.938             | —            | 0.265        | —            | —                                                             | —                                                             | —                                                             |  |  |
| 462904           | least altered           | residue  | 13.246                                  | 0.017            | 13.925                                  | 0.019            | 32.437                                  | 0.047            | 0.966             | 0.931             | 0.062        | 0.135        | 2.30         | 11.786                                                        | 13.476                                                        | 30.856                                                        |  |  |
| 462945           | least altered           | residue  | 12.436                                  | 0.015            | 13.768                                  | 0.018            | 32.179                                  | 0.051            | 0.940             | 0.813             | 0.012        | 0.170        | 2.62         | 11.005                                                        | 13.327                                                        | 30.630                                                        |  |  |
| 462946           | least altered           | residue  | 12.295                                  | 0.012            | 13.722                                  | 0.016            | 31.994                                  | 0.044            | 0.930             | 0.804             | 0.036        | 0.198        | 4.20         | —                                                             | —                                                             | —                                                             |  |  |
| 462947           | least altered           | residue  | 12.199                                  | 0.006            | 13.698                                  | 0.008            | 31.932                                  | 0.024            | 0.961             | 0.930             | —            | 0.178        | —            | —                                                             | —                                                             | —                                                             |  |  |
| 462948           | least altered           | residue  | 12.181                                  | 0.011            | 13.651                                  | 0.014            | 31.985                                  | 0.042            | 0.904             | 0.747             | 0.031        | 0.229        | 3.91         | 10.764                                                        | 13.215                                                        | 30.450                                                        |  |  |
| 462949           | least altered           | residue  | 12.239                                  | 0.008            | 13.668                                  | 0.010            | 32.019                                  | 0.030            | 0.935             | 0.842             | 0.041        | 0.209        | 2.90         | 10.819                                                        | 13.231                                                        | 30.481                                                        |  |  |
| 462965           | least altered           | residue  | 12.418                                  | 0.013            | 13.763                                  | 0.016            | 32.332                                  | 0.042            | 0.942             | 0.869             | 0.011        | 0.043        | 1.27         | 10.985                                                        | 13.322                                                        | 30.779                                                        |  |  |
| 462966           | least altered           | residue  | 12.449                                  | 0.009            | 13.730                                  | 0.012            | 32.181                                  | 0.031            | 0.959             | 0.935             | —            | 0.082        | —            | 11.688                                                        | 13.495                                                        | 31.356                                                        |  |  |
| 462967           | least altered           | residue  | failed                                  | —                | —                                       | —                | —                                       | —                | —                 | —                 | 0.029        | 0.055        | 2.99         | —                                                             | —                                                             | —                                                             |  |  |
| 242717a          | least altered           | residue  | 12.375                                  | 0.009            | 13.824                                  | 0.012            | 32.311                                  | 0.033            | 0.960             | 0.868             | 0.023        | 0.076        | 2.93         | 10.941                                                        | 13.383                                                        | 30.758                                                        |  |  |
| 242719C          | least altered           | residue  | 12.466                                  | 0.008            | 13.815                                  | 0.011            | 32.355                                  | 0.030            | 0.939             | 0.871             | —            | 0.054        | 4.01         | 11.029                                                        | 13.373                                                        | 30.799                                                        |  |  |
| 242790a          | least altered           | residue  | 13.704                                  | 0.007            | 14.087                                  | 0.009            | 33.218                                  | 0.026            | 0.959             | 0.925             | —            | —            | —            | —                                                             | —                                                             | —                                                             |  |  |
| 242729           | variably altered        | residue  | 12.803                                  | 0.008            | 13.889                                  | 0.011            | 32.540                                  | 0.029            | 0.957             | 0.927             | —            | —            | —            | —                                                             | —                                                             | —                                                             |  |  |
| 242737           | variably altered        | residue  | 15.733                                  | 0.056            | 14.892                                  | 0.054            | 34.811                                  | 0.127            | 0.988             | 0.988             | —            | —            | —            | —                                                             | —                                                             | —                                                             |  |  |
| 242743           | variably altered        | residue  | 15.959                                  | 0.069            | 14.808                                  | 0.065            | 35.467                                  | 0.156            | 0.991             | 0.988             | —            | —            | —            | —                                                             | —                                                             | —                                                             |  |  |
| 243689           | variably altered        | residue  | 14.690                                  | 0.062            | 14.564                                  | 0.062            | 32.831                                  | 0.140            | 0.990             | 0.991             | —            | —            | —            | —                                                             | —                                                             | —                                                             |  |  |
| 462906           | variably altered        | residue  | 12.330                                  | 0.006            | 13.812                                  | 0.008            | 32.201                                  | 0.024            | 0.961             | 0.927             | —            | —            | —            | —                                                             | —                                                             | —                                                             |  |  |
| 242673B          | variably altered        | residue  | 14.038                                  | 0.065            | 14.483                                  | 0.068            | 33.259                                  | 0.157            | 0.988             | 0.983             | —            | —            | —            | —                                                             | —                                                             | —                                                             |  |  |
| 242727H          | variably altered        | residue  | 14.144                                  | 0.061            | 14.303                                  | 0.062            | 34.214                                  | 0.149            | 0.988             | 0.990             | —            | —            | —            | —                                                             | —                                                             | —                                                             |  |  |
|                  |                         |          |                                         |                  |                                         |                  |                                         |                  |                   |                   | average      | 0.030        | 0.154        | 2.51                                                          |                                                               |                                                               |  |  |

<sup>§</sup> Degree of alteration as specified by Polat et al. (2002).

\*\* r<sub>1</sub><sup>206</sup>Pb/<sup>204</sup>Pb vs. <sup>207</sup>Pb/<sup>204</sup>Pb error correlation (Ludwig, 1988).

†† r<sub>2</sub><sup>206</sup>Pb/<sup>204</sup>Pb vs. <sup>208</sup>Pb/<sup>204</sup>Pb error correlation (Ludwig, 1988).

† Errors are two standard deviations absolute (Ludwig, 1988).

\* *in situ* age corrections are for 3510 My, using average Pb, Th and U concentrations and λ<sup>238</sup>U = 1.55125 × 10<sup>-10</sup>y<sup>-1</sup>, λ<sup>235</sup>U = 9.8485 × 10<sup>-10</sup>y<sup>-1</sup> and λ<sup>232</sup>Th = 4.9475 × 10<sup>-11</sup>y<sup>-1</sup> (Steiger and Jäger, 1977).

# Concentrations are from Polat et al. (2002a).

## U concentration estimated to be a fourth of the respective Th concentration.

concentrations in these metabasalts, relative to elements considered relative immobile, such as for example Zr.

The intersection age of 3.47 Gy with the single stage evolution curve best fitted through a set of least radiogenic galena data from

Isua (Frei and Rosing, 2001) is too young compared with the inferred extrusion age of ca. 3.69–3.71 Gy (Nutman et al., 1997, 2002) for this suite. Likewise, a similar and too young intersection age results also for the MORB source mantle evolution line of

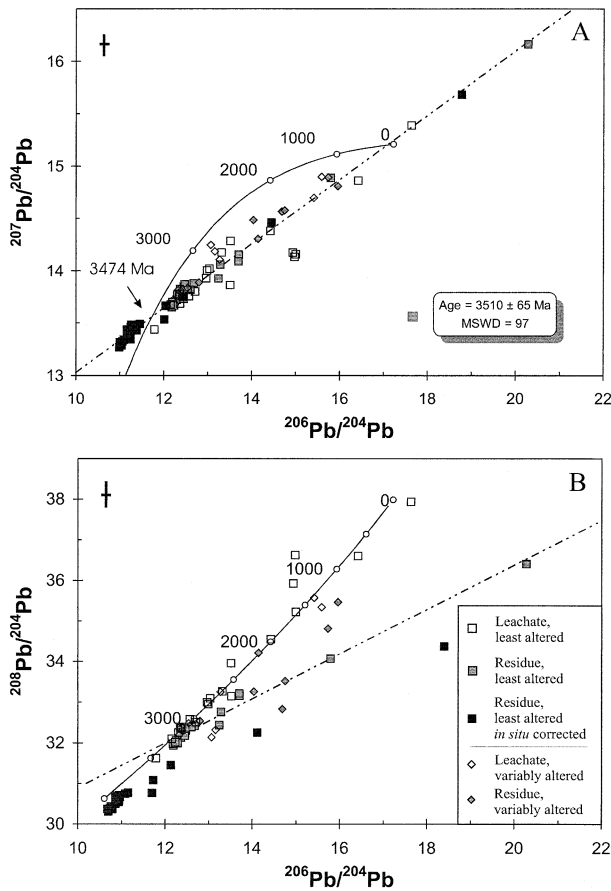


Fig. 5. (a) Uranogenic Pb isotope diagram with data from boninite-like metabasalts from the northeast central tectonic domain of the ISB. Samples termed “least altered” by Polat et al. (2002) show the smallest scatter and leached aliquots (residues; gray filled squares) define a correlation line with a slope corresponding to an age of  $3510 \pm 65$  My (MSWD = 97), which is interpreted as an Early Archean metamorphic resetting age. Gentle leaching of whole rock powders removed a Pb component of alteration (leachates; open squares), characterized by an increased thorogenic Pb component with higher  $^{208}\text{Pb}/^{204}\text{Pb}$  relative to  $^{206}\text{Pb}/^{204}\text{Pb}$  (see Fig. 5b). Reproducibility of data is indicated by the error cross in the upper left corners of the respective diagrams. The too young intersection age of 3474 Ma with the single stage Pb evolution line of Frei and Rosing (2001) indicates a high  $\mu$  component in the source of the rocks relative to contemporaneous mantle. This is also depicted by the bulk of in situ corrected data points (black filled squares), which plot significantly to the left and above the single stage mantle evolution line. (b) Uranogenic-thorogenic Pb isotope diagram. “Variably altered” samples are characterized by elevated thorogenic Pb relative to the samples termed “least altered” by Polat et al. (2002a). The correlation line through the “least altered” samples (residues; gray filled squares) indicates a component with high U/Pb relative to Th/Pb in the source of the boninite-like basalts, relative to contemporaneous mantle (characterized by the Pb evolution line of Frei and Rosing, 2001).

Kramers and Tolstikhin (1997) ( $^{238}\text{U}/^{204}\text{Pb} = 7.91$  at 4.55 Gy; not plotted here), which compares to the Frei and Rosing (2001) model with similar starting parameters ( $^{238}\text{U}/^{204}\text{Pb} = 7.70$  at 4.558 Ga). Using average concentrations, calculated from data reported by Polat et al. (2002a) for some “least altered” boninite-like metabasalts, for Pb =  $2.6 \pm 1.0$  ppm and Th =  $0.16 \pm 0.09$  ppm, and an estimated average U concentration of  $0.03 \pm 0.01$  ppm (U concentrations are not reported by Polat et al. (2002a) for

these rocks because they are close to the detection limit of the ICP-MS technique used), in situ corrected Pb isotopic compositions were computed using an age of metamorphism of 3.56 Gy (black filled squares in Fig. 5). The bulk of this data (15 out of 20 data points) plots to the left of the mantle evolution line of Frei and Rosing (2001) in Figure 5a. It records derivation of Pb from an environment that was characterized by a higher  $\mu$  value than contemporaneous mantle.

## 5. DISCUSSION

Although the literature on Hadean/Early Archean mantle derived rocks is extensive (for excellent reviews we refer to, e.g., Kramers, 2001, and Lewis and Knell, 2001, and references therein) the geochemical characterization of the Hadean mantle is at an “early” stage. This is due both to the scarcity of available rocks of this old age and, as discussed in the introduction, the modification of initial geochemical parameters by, often pervasive, postformation alteration processes. However, despite these obstacles, the emerging consensus is that the Hadean upper mantle underwent a complicated time-integrated evolution that seems to have included processes such as melt extraction (i.e., crust formation, with corresponding magmatic fractionations of compatible and incompatible elements) and subsequent recycling of crustal components back into previously depleted regions of the upper mantle (Bennett et al., 1993; McCulloch and Bennett, 1994). Attempts to understand these early mantle-crust processes naturally draw heavily on the analogy with modern plate tectonics and the geochemistry of existing rock types from the crust and the upper mantle. Detailed geochemical modeling of Hadean mantle processes therefore invariably come to rest on the assumption that existing crustal components are representative of the earliest mantle-crust system. This general assumption is, of course, debatable (e.g., Wilson et al., 2003). Our objective is therefore not to engage in detailed geochemical modeling of possible mixing relationships in the Hadean mantle, which would be based on speculative end-member compositions. Instead, we discuss our multi-isotopic data set from ISB boninite-like metabasalts in conjunction with the steadily expanding data base on Hadean/Early Archean mantle-derived materials with the aim to obtain, qualitatively, an idea of the types of processes and materials that was involved in the formation of these rocks and in the evolution of their mantle source region.

The results of this study emphasize the reality of what can be referred to as the “Hadean upper mantle conundrum,” by providing unambiguous isotopic evidence for the existence of a simultaneously depleted and enriched domain in the Early Archean and Hadean upper mantle (Bennett et al., 1993; McCulloch and Bennett, 1994; Wilson et al., 2003 and others). In the following, we first discuss evidence for source region depletion, which is based primarily on Sm-Nd systematics. Then we discuss Re-Os and Pb isotopic evidence for source region enrichment. Finally, we briefly discuss qualitatively two alternative geological processes that might provide at least part of the answer to the fascinating challenge that the Hadean upper mantle represents.

### 5.1. Evidence for the Existence of Depleted Upper Mantle before 3.7 Ga

Evidence for the existence of depleted upper mantle regions in the Early Archean and Hadean upper mantle comes mainly from the interpretation of Sm-Nd isotopic data (Bennett et al., 1993; McCulloch and Bennett, 1994; Wilson et al., 2003 and others). A large variation among reported initial  $\epsilon\text{Nd}$  values of supracrustal rocks and of encasing metagranitoids from the Isua area, has led to some debate. However, there now seem to be growing consensus that much of this “heterogeneity” can be attributed to postformational alteration processes, including tectono- metamorphic overprinting and hydrothermal metasomatic fluid interaction, both occurring during the Early and Late Archean. These events caused severe disturbance of mainly LREE systematics in rocks with low overall REE budgets, such as metabasalts and banded iron formations from within the ISB (e.g., Rosing, 1990; Gruau et al., 1996; Moorbath et al., 1997; Frei et al., 1999, 2002; Polat et al., 2002a,b, and many more). However, screening of rocks for minimum alteration, such as for example done by Bennett et al. (1993), Gruau et al. (1996) and Polat et al. (2002a,b) has resulted in a more consistent picture regarding the REE systematics of metabasalts from Isua, and has thus led the way to a better characterization of the mantle sources for these rocks. The agreement between the  $3.69 \pm 0.18$  Gy Sm-Nd age and the  $3.76 \pm 0.09$  Gy Re-Os age, and the accordance of these ages with the proposed emplacement age of 3.69–3.71 Gy (Nutman et al., 1997; Nutman et al., 2002) for this volcanic suite suggests that, in general, the Sm-Nd and Re-Os system in these metabasalts remained relatively and essentially undisturbed on the whole rock scale, respectively.

It has become increasingly clear that the mantle source of the ISB metabasalts was indeed characterized by long-term depletion. Bennett et al. (1993) reported positive initial  $\epsilon\text{Nd}$  values for nine out of 14 early Archean metagranitoids from southern West Greenland, implying that these rocks were derived from a LREE depleted mantle reservoir with an  $\epsilon\text{Nd}$  value of  $\sim +4$  before 3.8 Ga. Bennett et al.’s (1993) data set provided the best-constrained evidence for the existence of highly LREE fractionated mantle reservoirs in the early Earth. In combination with data from western Australia and southern Africa, Bennett et al. (1993) interpreted their Archean Nd isotope data to record isolation, depletion by crustal extraction and subsequent partial rehomogenization of limited portions of the upper mantle. Alternatively, they proposed a transient large-scale differentiation process unrelated to crustal extraction such as might occur in a terrestrial magma ocean.

The Sm-Nd data presented in this study also point to a depleted upper mantle reservoir for the source of the  $\sim 3.71$  Ga old boninite-like metabasalts from the central domain of the ISB. The average  $\epsilon\text{Nd}$  [ $T = 3.71$  Ga] whole rock value of  $+2.2 \pm 0.9$  from “least altered” boninite-like metabasalts from the northeast part of the ISB agrees with the value of  $2.5 \pm 0.4$  for such metabasalts from the W part and is in agreement with best estimates of  $\epsilon\text{Nd}$  [ $T = 3.85$  Ga] of  $\sim +2 \pm 2$  for the Isua mantle protolith (Blichert-Toft et al., 1999). Our initial values also are compatible with the value of  $\sim +2$  proposed by Gruau et al. (1996) for the “Garbenschiefer” metavolcanics. Furthermore, the initial Nd values of the boninite-like metabasalts compare

well with the average initial  $\epsilon\text{Nd}$  [ $T = 3.81$  Ga] value of  $2.6 \pm 1.6$  from “least altered” arc-like, picritic metabasalts from the older metavolcanic suite in the western part of the ISB (this study; Table 1). These older, arc-like metabasalts have higher Sm and Nd concentrations (Fig. 3) and therefore are less likely to have been affected by postformational alteration. In combination with the observation that boninite-like metabasalts define a nice correlation line (not good enough to be considered a true isochron) in a Sm-Nd isotope diagram with a slope corresponding to an early Archean age (Fig. 2), this supports the interpretation that the observed radiogenic initial  $^{143}\text{Nd}/^{144}\text{Nd}$  ratios are a primary signature.

The Nd isotopic compositions of modern boninites and arc basalts, even intraoceanic ones, are never as depleted as most Mid Ocean Ridge Basalts (MORB). If the ISB metabasalts are ancient arc basalt analogues (see below), they most likely have lower initial  $\epsilon\text{Nd}$  values than the unmetasomatized Early Archean upper mantle. Therefore it is reasonable to expect that 3.71 Ga, the upper mantle source region for the boninite-like metabasalts included a depleted component with an even higher initial  $\epsilon\text{Nd}$ , perhaps  $> \sim +3$ . This inference corroborates the proposal of Bennett et al. (1993) that the Earth’s mantle experienced Sm/Nd fractionation during a differentiation process very early in its history, consistent with evidence for the presence of live  $^{142}\text{Nd}$  in early Archean metabasalts (Boyet et al., 2002) and metasediments (Caro et al., 2003), following earlier evidence presented by Harper and Jacobsen (1992). Caro et al. (2003) constrained this event to  $4.460 \pm 0.115$  Ga, which makes it overlap with the final stages of terrestrial accretion. Furthermore, based on coupled  $^{147}\text{Sm}$  and  $^{146}\text{Sm}$  systematics, it was proposed that the enriched components were not recycled until  $\sim 4$  Ga (Harper and Jacobsen, 1992). These considerations suggest that Hadean upper mantle underwent a strong and early depletion event, which most likely left the upper protomantle substantially enriched in compatible elements, a prerequisite for explaining the high Mg-numbers and the elevated Cr and Ni contents observed in the metabasalts (Polat et al., 2002a) that formed during the early Archean. Subsequent modification of this depleted mantle by the addition of Th-, LREE- and Zr-enriched- but Nb-depleted, fluids or melts seem to have happened in the time interval between this primary depletion event and the second melt extraction event that led to the formation of the ISB metabasalts 3.71 Ga, or during the melting event itself.

Our Sm-Nd isotopic constraints stand in contrast to a recent study of Polat et al. (2002b), in which these authors reported Sm-Nd (and Rb-Sr) data on a set of pillow basalt rims and cores from the same metavolcanic suite and found them to be consistent with resetting of these isotope systems during Late Archean and Early to Mid-Proterozoic tectonothermal metamorphic events recorded in the region. It remains to be investigated in detail why Sm-Nd isotope data obtained on metabasalts from within the same lithological unit, from adjacent lithological units and from metabasalts in the western part of the ISB (Hamilton et al., 1983; Baadsgaard et al., 1986; Moorbath et al., 1986, 1997; Jacobsen and Dymek, 1988; Blichert-Toft et al., 1999) yield Early Archean isochron ages. Polat et al. (2002b) suggested that distinct chemical compositions and physical structures of the pillow rims and cores may have played a crucial role for the open system behavior of

Sm-Nd isotopes in these samples during Late Archean metamorphism.

## 5.2. Evidence for the Existence of Enriched Components before 3.7 Ga

### 5.2.1. Re-Os Isotopes

The agreement between the Re-Os isochron age and indirect age constraints from SHRIMP U-Pb zircon geochronological data from metagranitoid sheets emplaced within the metavolcanic sequences suggests a formation age of  $\sim 3.71$  Ga (Nutman et al., 1997) and indicates that the Re-Os isotopic system of these metabasalts in the low strain zones of the northeast central tectonic domain have remained essentially undisturbed. In addition, the depletion event identified by the positive  $\epsilon_{\text{Nd}}$  values for the source of the boninite-like metabasalts from the ISB is consistent with their very high Os concentrations. High concentrations of compatible elements (e.g., PGE) in a melt require a high degree of partial melting, which is likely to have been common in the Early Archean–Hadean upper mantle because of a higher heat production rate (e.g., Nisbet et al., 1993).

The Os isotopic signature ( $\gamma_{\text{Os}} = +4.4 \pm 1.2$ ) in the boninite-like metabasalts represents the first observation of distinctly radiogenic upper mantle component in the Early Archean–Hadean upper mantle. It imposes important constraints on their source regions by requiring mixing into the upper mantle source of material with a long-term suprachondritic Re/Os and, at the same time, with Os concentrations high enough to be an effective mixing component in the upper mantle. Based on enriched  $^{187}\text{Os}/^{188}\text{Os}$  ratios in peridotites from the Cascade arc (USA) and in the Japan Arc, Brandon et al. (1996) have shown that metasomatic reactions with fluids extracted from subducting oceanic crustal slabs and associated sediments can imprint radiogenic Os isotopic signatures on the resulting hybrid rocks, provided that these rocks are characterized by sufficiently low Os concentrations. However, the boninite-like metabasalts in this study are characterized by very high Os concentrations (1.7–3.7 ppb) and, because of the strongly compatible behavior of Os during partial melting, their upper mantle source region was likely characterized by a similar, if not higher, average Os concentration. Thus, the upper mantle source region of the boninite-like metabasalts would have been difficult to affect with radiogenic Os derived from a subducting slab similar to modern oceanic crust and sediments (Walker and Nisbet, 2002).

Recycling of a Hadean oceanic protocrust consisting of komatiite-like and basaltic components with a residence time of 700 Ma (the largest possible) into a primitive mantle is capable of explaining the radiogenic Os in the boninite-like metabasalts with  $\sim 30\%$  by mass of such a recycled crustal component (Puchtel and Humayun, 2001b). However, the major and trace element chemistry of these boninite-like metabasalts is not consistent with such proportions of recycled basaltic crust. Calculations summarized in Table 4 show that geologically unreasonable large proportions ( $\sim 95\%$  by mass) of such recycled oceanic crust are required to match the MgO and Ni contents of the boninite-like metabasalts, in turn leaving the Os and Re concentrations of the mantle reservoir too low and too

Table 4. Effect of assimilation of basaltic crust by a primitive mantle source.

| Components                                    | MgO (wt%) | Ni (ppm) | Os (ppb) | Re (ppb) |
|-----------------------------------------------|-----------|----------|----------|----------|
| Primitive mantle <sup>a</sup>                 | 37.8      | 2080     | 3.3      | 0.26     |
| Archean komatiite-basaltic crust <sup>b</sup> | 9.2       | 241      | 0.2      | 0.96     |
| 28% admixture of basaltic crust               | 29.8      | 1565     | 2.4      | 0.46     |
| 95% admixture of basaltic crust               | 10.6      | 333      | 0.4      | 0.93     |
| boninite-like metabasalts <sup>c</sup>        | 11.0      | 250      | 2.7      | 0.51     |

<sup>a</sup> From Puchtel and Humayun (2001b).

<sup>b</sup> From Puchtel and Humayun (2001b), calculated using compositions of the Kostomuksha komatiite liquid and average basalt composition mixed in the proportion 1:10.

<sup>c</sup> Average values for MgO and Ni computed from data in Polat et al. (2002a) and for Os and Re from this study (Table 3).

high, respectively. It is therefore difficult to explain the observed radiogenic Os in these metabasalts as a result of recycling of aged basaltic-komatiitic crust.

Alternatively, it has been suggested that back-mixing of outer core material might have affected the HSE budget of the upper mantle through time (e.g., Snow and Schmidt, 1998; Richter et al., 2000; Walker, 2000). This idea relies upon whole mantle convection, or deep-rooted mantle plumes to transport dissolved PGE from the core-mantle boundary to the upper mantle. Walker et al. (1995) proposed that the outer core could have developed radiogenic  $^{187}\text{Os}/^{188}\text{Os}$  as a result of Re-Os fractionation during inner core growth, and suggested that radiogenic Os isotopic compositions in some oceanic island basalts could be interpreted as a signature of core-mantle interaction and transport of radiogenic outer core Os to the upper mantle in deep rooted mantle plumes. Employing the assumption that portions the Hadean mantle did experience some kind of enrichment by radiogenic Os from the early outer core, we can compare our initial Os isotopic ratios with the suggested outer core Os isotopic evolution scenarios. The Re-Os isotopic data from this study (initial  $\gamma_{\text{Os}} = +4.4 \pm 1.2$ ) would require that the inner core started growing, and grew to its present size, within a time interval of less than 200 My after the accretion of the Earth. This result is illustrated in Figure 6, which shows the Os isotopic evolution of the outer core in models assuming different inner core growth histories and based on estimated solid/liquid partitioning coefficients for Re and Os at the inner core/outer core interface (Brandon et al., 2003). Because such extremely early inner core formation is geophysically implausible (e.g., Stacey and Loper, 1988; Labrosse et al., 1997; Labrosse et al., 2001), an outer core origin of the radiogenic Os isotopic signatures in the boninitic metabasalts can be ruled out.

### 5.2.2. Pb Isotopes

Whole rock Pb isotopic data indicate that the U-Th-Pb system was disturbed in the boninite-like metabasalts from Isua. It appears that nearly complete rehomogenization (accompanied by minor Pb loss) of the system occurred during Early Archean regional metamorphism ca. 3.56–3.58 Ga (Nutman et al., 2002). In Figure 7 data from the boninite-like suite are plotted together with the reference line defined by magnetite step-leaching data from BIF (Frei et al., 1999a) from within the

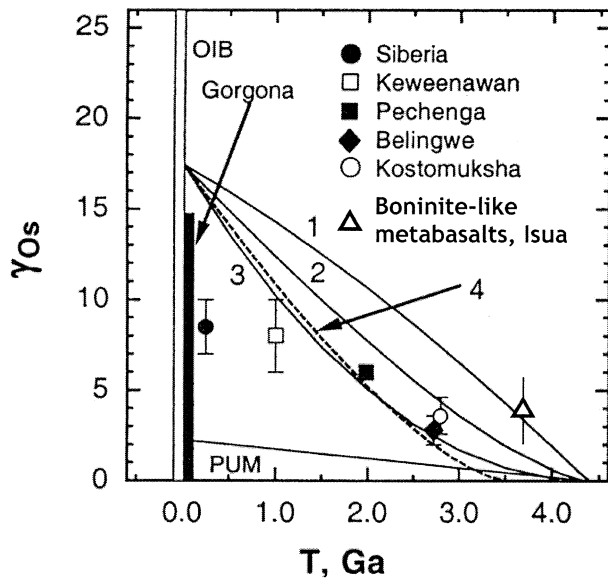


Fig. 6. Time versus  $\gamma_{Os}$  diagram (adapted from Brandon et al., 2003) with four different inner core evolution model lines. 1, Rapid growth; 2, intermediate growth; 3, constant growth; 4, intermediate delay start growth (as specified in table 2 of Brandon et al., 2003). The radiogenic average  $\gamma_{Os}$  value of  $+4.4 \pm 1.2$  ( $n = 8$ ;  $2\sigma$ ) of “least altered” boninite-like metabasalts from the northeast central tectonic domain of the ISB (open triangle) is plotted together with data from other locations (Brandon et al., 2003, and references therein). Only Model “1” (rapid inner core growth) is even remotely compatible with the radiogenic  $\gamma_{Os}$  values of the boninite-like metabasalts. But such rapid inner core growth is geophysically implausible. See text for discussion. PUM = primitive upper mantle (Meisel et al., 1996).

same central tectonic domain, and with the reference line defined by the  $>3.81$  Gy old metabasalts from the outer tectonic domain in the western part of the ISB (Frei et al., 2002). There is a marked difference in growth curve intersection ages between the older metabasalts from within the outer tectonic domain (“Amphibolite Unit”) and the metabasalts and associated BIF from central tectonic domain (“Garbenschiefer Unit”). The latter have too low intersection ages for Pb to have been extracted from a mantle with a single stage evolution, such as that proposed by Frei and Rosing (2001; solid evolution line). Kamber et al. (2003) elaborated on the problem of too low radiogenic intersection criteria (nominal age of 3.69 Gy) for feldspar data from the 3.81 Ga Tonalite-Trondhjemite-Granite (TTG) gneisses from the area south of the ISB with single stage mantle growth curves. These authors noticed a good fit between a modelled 4.3 Gy basaltic protocrust evolution line (with a  $\mu$  value, i.e.,  $^{238}U/^{204}Pb$  ratio, of 10.5; plotted as a dashed evolution line in Fig. 7) and initial isotope ratios from TTGs, BIF and metapelites from the ISB and the area south of it (Kamber et al., 2003). A similar case (intersection age of 3868 Ma with the protocrust evolution line) is obtained with the  $>3.81$  Ga metabasalts from the outer tectonic domain in the W part of the ISB (Frei et al., 2002). The difference in  $^{207}Pb/^{204}Pb$  between the 3.47 Ga intersection age (Fig. 7) of the boninite-like metabasalt suite and their inferred  $\sim 3.71$  Ga extrusion age is substantial. A simple two stage process in which the U-Th-Pb isotopic system was effectively opened on a whole rock scale during a single metamorphic event at 3560 Ma cannot explain

the too young intersection age of these rocks with single mantle evolution lines. If the whole rock Pb isotope array was formed in multiple events of incomplete homogenization, it may have experienced some clock-wise rotation, resulting in an artificially “young” intersection with mantle evolution curves. However, the proximity of the bulk of residue data points (15 out of 20) to the single stage mantle evolution curve of Frei and Rosing (2001) renders the intersection ages relatively inert to regression slope variations, even if the two most radiogenic data points, which dominate the slope of the correlation line (Figs. 5a and 8), are excluded. We therefore consider the difference in  $^{207}Pb/^{204}Pb$  between 3.71 Ga and 3.47 Ga robust and well outside any regression uncertainty, implying that the source evolved for some time with a significantly higher U/Pb ratio than the contemporaneous mantle. This is supported by the bulk of in situ growth corrected data points, which plot significantly to the right of the single stage mantle evolution line (Figs. 5a and 7).

Adopting the protocrust model of Kamber et al. (2003), the correlation line defined by boninite-like metabasalt samples intersects at 3708 Ma (Fig. 7), in accordance with their assumed formation age. This result is consistent with other intersection parameters from main lithological units from within the ISB using the same model, including Pb isotope data of galena from the ISB (e.g., Richards and Appel, 1987; Frei et al., 1999b; Kamber et al., 2003), data from BIF genetically associated with the boninite-like metabasalts from the central tec-

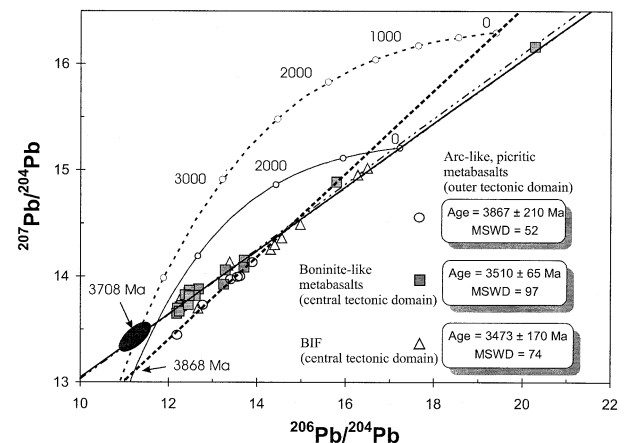


Fig. 7. Uranogenic Pb isotope diagram with data of boninite-like metabasalts (this study; gray filled squares, solid correlation line), arc-like, picritic metabasalts from the outer tectonic domain in the western part of the ISB (Frei et al., 2002; open circles; dashed correlation line) and of BIF from the northeast central tectonic domain of the ISB (Frei et al., 1999; open triangles, dash-dotted correlation line). While the correlation lines of boninite-like metabasalts and BIF intersect the single stage Pb isotope evolution line of Frei and Rosing (2001) at too young model ages, the intersection at 3708 Ma with a recently proposed protocrustal evolution line (Kamber et al., 2003), with separation from the mantle 4.3 Ga and a  $\mu$ -value of 10.5, is in good agreement with the proposed extrusion age of  $\sim 3.71$  Gy (Nutman et al., 1997). The main cluster of in situ corrected data points (outlined by black-filled ellipse) of boninite-like metabasalts plots to left of the Frei and Rosing (2001) mantle evolution, but on the proposed protocrustal line of Kamber et al. (2003). In combination with the lower (i.e., older) intersection age defined by the older arc-like metabasalts, the data of boninite-like metabasalts and BIF indicates admixing of a high- $\mu$  Hadean Pb component into their mantle source before their formation.

tonic domain of the ISB (Moorbath et al., 1973; Frei et al., 1999a), and data from older (>3.81 Ga) metabasalts from the outer tectonic domain (Frei et al., 2002). All the Pb isotopic data from these lithological units, and the boninite-like metabasalts studied by us, require an elevated  $\mu$ -value in their source region, compared with normal mantle evolution models.

The lack of correlation of Pb concentrations with immobile elements such as Zr in these boninite-like metabasalts (Polat et al., 2002a, their fig. 2g), combined with the Pb isotope systematic discussed above, suggest that Pb-loss (rather than gain by hydrothermal-metasomatic processes) during a  $\sim$ 3.56 Gy old metamorphic event was the major process disturbing the U-Th-Pb isotope systematics and Pb budgets in these rocks. Therefore, we consider the measured Pb concentrations to be minimum values. However, in comparison with the average Pb concentrations of the extremely incompatible-element depleted to less depleted boninites from the Ordovician Betts Cove ophiolite (Newfoundland; Bédard, 1999), which range from 0.3 to 1.1 ppm (average  $0.7 \pm 0.3$ ), the average Pb concentration of  $2.6 \pm 0.9$  ppm (calculated from data in Polat et al., 2002a; their table 2) for the boninite-like metabasalts is still very high. Normalized against N-MORB (Sun and McDonough, 1989), the measured Pb/Nd ratios in the boninite-like metabasalts studied herein (average Pb/Nd<sub>N</sub>  $\sim$ 39, calculated from data in Polat et al., 2002a; their table 2) are about twice as high as those of boninites from Betts Cove (average Pb/Nd<sub>N</sub>  $\sim$ 19; calculated from data in Bédard, 1999; his table 2). This strong enrichment in Pb is in agreement with the isotopic evidence for the involvement of substantial amounts of high- $\mu$  sediment components in the source of the metabasalts.

### 5.3. Plausible Geological Scenarios

Polat et al. (2002a) have described the geochemistry of the metabasalts from the “Garbenschiefer Unit,” which dominate the central tectonic domain of the ISB (Fig. 1). These rocks are characterized by high MgO (7–18 wt%), Ni (61–645 ppm), and Cr (61–1920 ppm), moderate variations in Al<sub>2</sub>O<sub>3</sub> (14–20 wt%) and SiO<sub>2</sub> (47–54 wt%), but low TiO<sub>2</sub> (0.20–0.40 wt%), Zr (12–30 ppm) and rare earth element (REE) concentrations. These compositional features collectively define a basaltic to high-MgO basaltic suite. The metabasalts are furthermore characterized by depleted to enriched LREE and negatively fractionated HREE patterns. MREEs are consistently depleted relative to neighboring REEs. In addition, they exhibit variably large negative Nb, variably positive Zr and negative to positive Ti anomalies, relative to primitive mantle normalized trace element patterns (Polat et al., 2002a). Based on the similarity of these geochemical signatures (specifically; low TiO<sub>2</sub>, Zr, and Nb contents, high Al<sub>2</sub>O<sub>3</sub>/TiO<sub>2</sub> ratios, positive anomalies of Zr with respect to neighboring REE, U-shaped LREE and fractionated HREE pattern), with fresh Tertiary boninites such as Bonin Islands (e.g., Taylor et al., 1994), Mariana trench (e.g., Stern et al., 1991) and ophiolitic low-Ti tholeiites such as Betts Cove (Bédard, 1999), Polat et al. (2002a) concluded that the metavolcanic rocks from the “Garbenschiefer Unit” are closely related to boninites. Collectively, these rocks were shown to exhibit geochemical characteristics that are very similar to those of Phanerozoic boninites, which suggest a subduction zone environment for their formation (Polat et al., 2002a).

Thus, while it is difficult to reconcile the combined isotopic Sm-Nd, Re-Os, and Pb isotopic signatures of the 3.71 Gy old boninite-like metabasalts with a simple recycling/mixing scenario involving a depleted mantle component and one or two enriched crustal component(s) with modern analogues, it seems clear that subduction zone processes and recycling of crustal components must have played key roles in the evolution of at least this part of the Hadean upper mantle.

Pb isotope systematics (due to their distinct radiogenic character in continental crust and its sedimentary deviates) and the high Pb concentrations argue for the involvement of substantial amounts of high- $\mu$ , high Pb sediment components in the source of the metabasalts. At the same time, recycling of reasonable proportions of modern or aged basaltic-komatiitic oceanic crust can not satisfactorily account for the radiogenic Os isotope systematics of this mantle source, which has preserved a Sm-Nd signature of strong and early depletion.

Indeed, the suprachondritic <sup>187</sup>Os/<sup>188</sup>Os ratios of the boninite-like metabasalts seem to require another process capable of creating high Re/Os reservoirs in the mantle. Two processes that might have been relevant to the Re-Os systematics of the Hadean upper mantle should be brought into attention:

Smith (2003) has suggested that partitioning of PGE into pyroxenites precipitated from Mg-rich, depleted mantle melts might be a plausible mechanism by which high Re/Os elemental ratios can be generated, which rapidly (on the order of tens of My) can evolve into strongly suprachondritic <sup>187</sup>Os/<sup>187</sup>Os domains in the upper mantle. Such pyroxenite lithologies could become important mixing components in a subsequent partial melting event (Carlson and Irving, 1994). On time scales characteristic of the Hadean crust-mantle system (i.e., from 4.4 to 3.9 Ga) there would have been more than enough time for radiogenic <sup>187</sup>Os/<sup>188</sup>Os signatures to develop in such pyroxenite lithologies in the shallow upper mantle. The high Mg content of Hadean basalts and the very large extent of melting generally implied for the Hadean upper mantle would be favorable to the formation of pyroxenite cumulates compared to the post-Hadean, and particularly, the Phanerozoic times. However, field evidence shows that vein-type pyroxenites and pyroxenite dikes usually constitute a very small proportion (<1%) of a total residual ophiolite sequence. Their PGE patterns are complementary to that in dunites, in which pyroxenites occur, and which show a strong depletion in Pt and Pd over Os and Ir. This is because pyroxenites and dunites are derived from host harzburgites as a result of melting/metasomatic processes, and harzburgites generally exhibit unfractionated PGE patterns. Richter et al. (2000) presented new data for PGE and Re partitioning between pyroxene and silicate melt. They found that Pt is only slightly compatible in pyroxene ( $D = 1.5$ ) and Re is incompatible. This would indicate that the high Pt and Re abundances in some ophiolitic pyroxenites, as reported by Smith (2003), could be the result of metasomatic processes and in situ PGE redistributions. Clearly, more analytical work is needed to better evaluate this model.

Another process potentially might also have played an important role. The Hadean crust was frequently bombarded by meteorites and small asteroids (Hartmann et al., 2000). It is therefore reasonable to consider the possibility that the sediments accumulated on the relatively stable Hadean crust could have acted as a repository for meteoritic debris, e.g., iron

meteorite material, which would be rich in PGE compared to the Hadean upper mantle and provide strongly radiogenic Os (Morgan, 1985; Shirey and Walker, 1998; Morgan et al., 2001). Furthermore, although the preferential release of Re from modern subducting sediments and oceanic crust is not believed to affect the Re-Os isotopic evolution of the overlying mantle wedge because these crustal components are, in general, poor in PGE (Walker and Nisbet, 2002; Walker et al., 2002), this does not necessarily hold true for subduction of a Hadean regolith with a large meteoritic component. Such a regolith might have had an enhanced potential for affecting the PGE systematics of a supra-subduction zone mantle wedge. Furthermore, because of a presumed high Pb/Nd ratio of the slab fluids, a result of the higher metasomatic fluid mobility of Pb compared with Nd, supra-subduction zone derived basalts could potentially carry a crustal/sediment Pb-isotopic signature while its Nd isotopic composition could remain dominated by the depleted upper mantle components.

## 6. SUMMARY AND CONCLUSIONS

The combined Sm-Nd, Re-Os and Pb isotopic investigation of a set of high-Mg, low-HFSE boninite-like metabasalts from the central tectonic domain of the northeast sector of the ISB has yielded the following results:

1. Despite various postformational metamorphic-metasomatic overprinting of the ISB, careful selection of the “least altered” (based on trace element criteria by Polat et al., 2002a) samples from low-strain zones still allows characterization of the mantle source(s) of these ~3.71 Ga old metabasalts. Our multi-isotopic data set relies on previously described main- and trace elemental alteration criteria, which allowed selection of samples with minimum major and trace elemental perturbations.

2. Nd isotope data confirm the existence of a highly depleted mantle source for the boninite-like metabasalts ( $\epsilon\text{Nd}[T = 3.71 \text{ Ga}] = +2.2 \pm 0.9$ ). Taking into account that the petrogenesis of these basalts is likely to have involved some components of recycled Hadean crust characterized by potentially radiogenic Nd isotopic signatures, this range in initial  $\epsilon\text{Nd}$  values is to be considered a minimum estimate for the mantle at the time of formation of these basalts (Bennett et al., 1993). Strong parent/daughter fractionation apparently occurred already early in the Hadean, consistent with the reported  $^{142}\text{Nd}$  excesses that require differentiation of the Earth’s mantle and crust formation no later than ~4.3 Ga ago (Harper and Jacobsen, 1992; Boyet et al., 2002; Caro et al., 2003).

3. Re-Os isotopic data of the boninite-like metabasalts, combined with their high Os concentrations, which are similar to those of the primitive mantle, indicate a suprachondritic mantle reservoir ( $\gamma\text{Os}[T = 3.71 \text{ Ga}] = 4.4 \pm 1.2$ ) and high degrees of melting capable of transferring large amount of PGEs into the basaltic melts. This is compatible with their overall high Mg, Cr and Ni concentrations.

4. Pb isotopes of the boninite-like metabasalts from Isua are comparable to the signatures observed in BIF (Moorbath et al., 1973; Frei et al., 1999a) and together with indications from a number of other rock associations, including pelitic metasediments and TTG gneisses from within the Isuakasia area (Kamber and Moorbath, 1998; Kamber et al., 2003) have too young

intersection ages with commonly used single stage mantle Pb evolution curves.

5. In combination with the implications from Sm-Nd and Re-Os systematics, our Pb isotopic data of the boninite-like metabasalts is consistent with the inferred existence of a Hadean (basaltic) protocrust that separated from the mantle at ~4.3 Ga ago (Kamber et al., 2003). The intersection criteria (high  $^{207}\text{Pb}/^{204}\text{Pb}$  relative to  $^{206}\text{Pb}/^{204}\text{Pb}$ ) for these metabasalts (and also for the older arc-like, picritic metabasalts from the outer/inner tectonic domain of the ISB) require a component derived from a high- $\mu$  protocrust ( $\mu = 10.5$ ).

6. No single recycled component seems to be capable of explaining all isotopic features. The role of pyroxene-rich lithologies in melt generation (Smith, 2003) and accumulation of PGE-rich meteoritic debris on the Hadean crust, subsequently recycled into the mantle, should be investigated as processes that could potentially have affected the PGE systematics of a supra-subduction zone mantle wedge to produce high Re/Os environments allowing for  $^{187}\text{Os}$  in-growth, even on relatively short time scales.

Our combined isotopic data show that by 3.7–3.8 Ga domains with complicated enrichment/depletion histories existed in the upper mantle. While the melt source of the boninite-like metabasalts appears geochemically enriched in the Pb and Os isotopic systems, it is depleted in the Nd isotopic system. We refer to these observations as the “Hadean upper mantle conundrum.” The solution to the conundrum is clearly multifaceted and highly complicated. However, both trace element and isotopic evidence seem broadly consistent with formation of the boninite-like metabasalts in an oceanic “subduction” environment in which Hadean crustal components, conceivably without any present-day analogues, were recycled following the establishment of subduction-like processes before ~3.7–3.8 Gy ago.

*Acknowledgments*—We thank John Bailey for an informal review. Birthe Møller and Maria Jankowski were a big help in processing the samples through the clean laboratories of the Geological Institute, University of Copenhagen. Minik Rosing provided us with a number of samples from Isua, for which we are very grateful. AP acknowledges the Isua Multi Disciplinary Research project and the NSERC grant 250926. We also thank V. C. Bennett, B. S. Kamber, and I. S. Puchtel for highly constructive reviews that greatly helped us to improve the manuscript. AM gratefully acknowledges NSF support through the award number EAR-0309414.

*Associate editor:* A. D. Brandon

## REFERENCES

- Appel P. W. U., Fedo C. M., Moorbath S., and Myers J. S. (1998) Recognizable primary volcanic and sedimentary features in a low-strain domain of the highly deformed, oldest known ( $\delta F$  3.7–3.8 Gyr) greenstone belt, Isua, West Greenland. *Terra Nova* **10**, 57–62.
- Arndt N. T., Albarède F., and Nisbet E. G. (1997) Mafic and ultramafic magmatism. In *Greenstone Belts* (eds. M. J. de Wit and L. D. Ashwal), pp. 233–254. Oxford Monographs on Geology and Geophysics 35.
- Baadsgaard H. (1983) U-Pb isotope systematics on minerals from the gneiss complex at Isukasia, West Greenland. Rapport Grønlands Geologiske Undersøgelse. *Rep. Geol. Surv. Greenland* **112**, 35–42.
- Baadsgaard H., Nutman A. P., Rosing M., Bridgwater D., and Longstaffe Fred J. (1986) Alteration and metamorphism of Amitsoq Gneisses from the Isukasia area, West Greenland; recommendations for isotope studies of the early crust. *Geochim. Cosmochim. Acta* **50**, 2165–2172.

- Bédard J. H. (1999) Petrogenesis of boninites from the Betts Cove ophiolite, Newfoundland, Canada: Identification of subducted source components. *J. Petrol.* **40**, 1853–1889.
- Bennett V. C., Nutman Allen P., and McCulloch Malcolm T. (1993) Nd isotopic evidence for transient, highly depleted mantle reservoirs in the early history of the Earth. *Earth Planet. Sci. Lett.* **119**, 299–317.
- Blichert-Toft J., Albarède F., Rosing M., Frei R., and Bridgwater D. (1999) The Nd and Hf isotope evolution of the mantle through the Archean; results from the Isua supracrustals, West Greenland, and from the Birimian terranes of West Africa. *Geochim. Cosmochim. Acta* **63**, 3901–3914.
- Boyett M., Albarède F., Télouk P., and Rosing M. (2002)  $^{142}\text{Nd}$  anomaly confirmed at Isua (abstract). In *Special Supplement, Abstracts of the 12th Annual V.M. Goldschmidt Conference, Davos, Switzerland* (August 18–23, 2002). *Geochim. Cosmochim. Acta* **66**, A99.
- Brandon A. D., Creaser R. A., Shirey S. B., and Carlson R. W. (1996) Osmium recycling in subduction zones. *Science* **272**, 861–864.
- Brandon A. D., Walker R. J., Puchtel I. S., Becker H., Humayun M., and Revillon S. (2003)  $^{186}\text{Os}$ – $^{187}\text{Os}$  systematics of Gorgona Island komatiites; implications for early growth of the inner core. *Earth Planet. Sci. Lett.* **206**, 411–426.
- Carlson R. W. and Irving A. J. (1994) Depletion and enrichment history of subcontinental lithospheric mantle: An Os, Sr, Nd and Pb isotopic study of ultramafic xenoliths from the northwestern Wyoming Craton. *Earth Planet. Sci. Lett.* **126**, 457–472.
- Caro G., Bourdon B., Bircck J.-L., and Moorbath S. (2003)  $^{146}\text{Sm}$ – $^{142}\text{Nd}$  evidence from Isua metamorphosed sediments for early differentiation of the Earth's mantle. *Nature* **423**, 428–432.
- Cohen A. S. and Waters F. G. (1996) Separation of osmium from geological materials by solvent extraction for analysis by thermal ionisation mass spectrometry. *Anal. Chim. Acta* **322**, 269–275.
- Frei R., Bridgwater D., and Rosing M. (1997) Apparent controversies of Pb–Pb and Sm–Nd isotope systematics in the Archean Isua (West Greenland) BIFs: Preservation of primary signatures vs. secondary disturbances. In *AGU 1997 Fall Meeting*, Vol. 78, 46 Suppl., p. 830.
- Frei R., Bridgwater D., Rosing M., and Stecher O. (1999a) Controversial Pb–Pb and Sm–Nd isotope results in the early Archean Isua (West Greenland) oxide iron formation; preservation of primary signatures versus secondary disturbances. *Geochim. Cosmochim. Acta* **63**, 473–488.
- Frei R., Rosing M. T., Krogstad E. J., Storey M., Ulfbeck D. G., and Albarède F. (1999b) The least radiogenic terrestrial Pb; its implications for the early Archean crustal evolution recorded in the Isua supracrustal belt (West Greenland). In *AGU 1999 Fall Meeting*, Vol. 80, 46 Suppl., pp. 1190–1191.
- Frei R. and Rosing M. T. (2001) The least radiogenic terrestrial leads; implications for the early Archean crustal evolution and hydrothermal-metasomatic processes in the Isua supracrustal belt (West Greenland). *Chem. Geol.* **181**, 47–66.
- Frei R., Rosing M. T., Waight T. E., and Ulfbeck D. G. (2002) Hydrothermal-metasomatic and tectono-metamorphic processes in the Isua supracrustal belt (West Greenland); a multi-isotopic investigation of their effects on the Earth's oldest oceanic crustal sequence. *Geochim. Cosmochim. Acta* **66**, 467–486.
- Frei R. and Kastbjerg Jensen B. (2003) Re–Os, Sm–Nd isotope and REE systematics on ultramafic rocks and pillow basalts from the Earth's oldest oceanic crustal fragments (Isua Supracrustal Belt and Ujargssuit nunât area, W Greenland). *Chem. Geol.* **196**, 163–191.
- Gruau G., Rosing M., Bridgwater D., and Gill R. C. O. (1996) Resetting of Sm–Nd systematics during metamorphism of >3.7-Ga rocks; implications for isotopic models of early Earth differentiation. *Chem. Geol.* **133**, 225–240.
- Hamilton P. J., O'Nions R. K., Bridgwater D., and Nutman A. (1983) Nd-isotope studies of Archean metasediments and metavolcanics from West Greenland and their implications for the early Earth history. *Earth Planet. Sci. Lett.* **9**, 269–279.
- Harper C. L. and Jacobsen S. B. (1992) Evidence from coupled  $^{147}\text{Sm}$ – $^{143}\text{Nd}$  and  $^{146}\text{Sm}$ – $^{142}\text{Nd}$  systematics for very early (4.5-Gyr) differentiation of the Earth's mantle. *Nature* **360**, 728–732.
- Hartmann W. K., Ryder G., Dones L., and Grinspoon D. (2000) The time-dependent intense bombardment of the primordial Earth/Moon system. In *Origin of the Earth and the Moon* (eds. R. M. Canup and K. Righter), 555. University of Arizona Press.
- Jacobsen S. B. and Dymek R. F. (1988) Nd and Sr isotope systematics of clastic metasediments from Isua, West Greenland: Identification of pre-3.8 differentiated crustal components. *J. Geophys. Res.* **93**, 338–354.
- Jochum K. P., Arndt N. T., and Hofmann A. W. (1991) Nb–Th–La in komatiites and basalts: Constraints on komatiite petrogenesis and mantle evolution. *Earth Planet. Sci. Lett.* **107**, 272–289.
- Kamber B. S. and Moorbath S. (1998) Initial Pb of the Amitsoq Gneiss revisited; implication for the timing of early Archean crustal evolution in West Greenland. *Chem. Geol.* **150**, 19–41.
- Kamber B. S., Colerson K. D., Moorbath S., and Whitehouse M. J. (2003) Inheritance of early Archean Pb-isotope variability from long-lived Hadean protocrust. *Contrib. Mineral. Petrol.* **145**, 25–46.
- Komiya T. and Maruyama S. (1995) Geochemistry of the oldest MORB and OIB of the World, Isua (3.8 Ga), Greenland. In *AGU 1994 Fall Meeting*, Vol. 75, 44 Suppl., p. 691.
- Kramers J. D. (2001) The smile of the Cheshire cat. *Science* **293**, 619–620.
- Kramers J. D. and Tolstikhin I. N. (1997) Two Terrestrial Lead Isotope Paradoxes, Forward Transport Modelling, Core Formation and the History of the Continental Crust. *Chem. Geol.* **139**, 75–110.
- Labrosse S., Poirier J.-P., and LeMouél J.-L. (1997) On cooling of the Earth's core. *Phys. Earth Planet. Interiors* **99**, 1–17.
- Labrosse S., Poirier J.-P., and LeMouél J.-L. (2001) The age of the inner core. *Earth Planet. Sci. Lett.* **190**, 111–123.
- Lewis C. L. E. and Knell S. J. (2001) *The Age of the Earth: From 4004 BC to AD 2002*. Publication 190. Geological Society of London.
- Ludwig K. R. (1988) A computer program to convert raw U–Th–Pb isotope ratios to blank-corrected isotope ratios and concentrations with associated error-correlations. Open File Report OF-82-820. U.S. Geological Survey.
- Maruyama S., Masuda T., Nohda S., and Appel P. (1992) The earliest records on oceanic and continental crusts from 3.8 Ga accretionary complex, Isua, Greenland. In *29th International Geological Congress, Kyoto, Japan* (August 24–September 3, 1992). Abstract Suppl. 29, p. 5.
- McCulloch M. T. and Bennett V. C. (1994) Progressive growth of the Earth's continental crust and depleted mantle; geochemical constraints. *Geochim. Cosmochim. Acta* **58**, 4717–4738.
- Meisel T., Walker R. J., and Morgan J. W. (1996) The osmium isotopic composition of the Earth's primitive upper mantle. *Nature* **383**, 517–520.
- Meisel T., Walker R. J., Irving A. J., and Lorand J. P. (2001) Osmium isotopic compositions of mantle xenoliths; a global perspective. *Geochim. Cosmochim. Acta* **65**, 1311–1323.
- Moorbath S., O'Nions R. K., and Pankhurst R. J. (1973) Early Archean age for the Isua Iron Formation, West Greenland. *Nature* **245**, 138–139.
- Moorbath S., Taylor P. N., and Jones N. W. (1986) Dating the oldest terrestrial rocks – fact and fiction. *Chem. Geol.* **135**, 213–231.
- Moorbath S., Whitehouse M. J., and Kamber B. S. (1997) Extreme Nd isotope heterogeneity in the Early Archean: Fact or fiction: Case histories from Northern Canada and West Greenland. *Chem. Geol.* **135**, 213–231.
- Morgan J. W. (1985) Osmium isotopic constraints on Earth's late accretionary history. *Nature* **317**, 703–705.
- Morgan J. W., Walker R. J., Brandon A. D., and Horan M. F. (2001) Siderophile elements in Earth's upper mantle and lunar breccias: Data synthesis suggests manifestations of the same late influx. *Meteor. Planet. Sci.* **36**, 1257–1275.
- Myers J. S. (2002) Protoliths of the 3.8–3.7 Ga Isua greenstone belt, West Greenland; reply. *Precamb. Res.* **117**, 151–156.
- Nägler T. F. and Frei R. (1997) Plug in plug osmium distillation. *Schweiz. Mineral. Petrograph. Mitteilungen* **76**, 123–127.
- Nisbet E. G., Cheadle M. J., Arndt N. T., and Bickle M. J. (1993) Constraining the potential temperature of the Archean mantle: A review of the evidence from komatiites. *Lithos* **30**, 291–307.
- Nutman A. P., Bennett V. C., Friend C. R. L., and Rosing M. T. (1997) Approximately ~3710 and >3790 Ma volcanic sequences in the Isua (Greenland) supracrustal belt; structural and Nd isotope implications. *Chem. Geol.* **141**, 271–287.
- Nutman A. P., Friend C. R. L., and Bennett V. C. (2002) Evidence for 3650–3600. Ma assembly of the northern end of the Itsaq gneiss complex, Greenland; implication for early Archean tectonics. *Tectonics* **21**, 10.1029/2000TC001203.
- Polat A., Hofmann A. W., and Rosing M. T. (2002a) Boninite-like volcanic rocks in the 3.7–3.8 Ga Isua greenstone belt, West Green-

- land; geochemical evidence for intra-oceanic subduction zone processes in the early Earth. *Chem. Geol.* **184**, 231–254.
- Polat A., Hofmann A. W., Münker C., Regelous M., and Appel P. W. U. (2002b) Contrasting geochemical pattern in the 3.7–3.8 Ga pillow basalt cores and rims, Isua greenstone belt, southwest Greenland: Implications for postmagmatic alteration processes. *Geochim. Cosmochim. Acta* **67**, 441–457.
- Polat A. and Hofmann A. W. (2003) Alteration and geochemical patterns in the 3.7–3.8 Ga Isua greenstone belt, West Greenland. *Precamb. Res.* **126**, 197–218.
- Puchtel I. S., Hofmann A. W., Mezger K., Jochum K. P., Schipansky A. A., and Samsonov S. V. (1998) Oceanic plateau model for continental crustal growth in the Archean: A case study for the Kostomuksha greenstone belt, NW Baltic Shield. *Earth Planet. Sci. Lett.* **155**, 57–74.
- Puchtel I. S. and Humayun M. (2000) Platinum group elements in Kostomuksha komatiites and basalts; implications for oceanic crust recycling and core-mantle interaction. *Geochim. Cosmochim. Acta* **64**, 4227–4242.
- Puchtel I. S. and Humayun M. (2001a) Platinum group element fractionation in a komatiitic basalt lava lake. *Geochim. Cosmochim. Acta* **65**, 2979–2993.
- Puchtel I. S. and Humayun M. (2001b)  $^{187}\text{Os}$ -enriched domain in an Archean mantle plume: Evidence from 2.8 Ga komatiites of the Kostomuksha greenstone belt, NW Baltic shield. *Earth Planet. Sci. Lett.* **186**, 513–526.
- Richards J. R. and Appel P. W. U. (1987) Age of the “least radiogenic” galenas at Isua, West Greenland. *Chem. Geol.* **66**, 181–191.
- Righter K., Walker R. J., and Warren P. H. (2000) Significance of highly siderophile elements and osmium isotopes in the lunar and terrestrial mantles. In *Origin of the Earth and Moon* (eds. R. M. Canup and K. Righter), pp. 291–322. The University of Arizona Press, Tucson.
- Rose N. M., Rosing M. T., and Bridgwater D. (1996) The origin of metacarbonate rocks in the Archaean Isua supracrustal belt, West Greenland. *Am. J. Sci.* **296**, 1004–1044.
- Rosing M. T. (1990) The theoretical effect of metasomatism on Sm-Nd isotopic systems. *Geochim. Cosmochim. Acta* **54**, 1337–1341.
- Rosing M. T., Rose N. M., Bridgwater D., and Thomsen H. S. (1996) Earliest part of Earth’s stratigraphic record; a reappraisal of the >3.7 Ga Isua (Greenland) supracrustal sequence. *Geology* **24**, 43–46.
- Rosing M. T. and Frei R. (1999) Late Archaean metasomatism and kyanite formation in the >3700 Ma Isua supracrustals, West Greenland (abstract). In *European Union of Geosciences Conference Abstracts, EUG 10*. Vol. 4, p. 144.
- Roy-Barman M. and Allègre C. J. (1994)  $^{187}\text{Os}/^{186}\text{Os}$  ratios of mid-ocean ridge basalts and abyssal peridotites. *Geochim. Cosmochim. Acta* **58**, 5043–5054.
- Schaller M., Steiner O., Studer I., Frei R., and Kramers J. D. (1997) Pb stepwise leaching (Pbsl) dating of garnet; addressing the inclusion problem. *Schweiz. Mineral. Petrogr. Mitteilungen* **77**, 113–121.
- Shimizu H., Umemoto N., Masuda A., and Appel P. W. U. (1990) Sources of iron-formations in the Archean Isua and Malene supracrustals, West Greenland; evidence from La-Ce and Sm-Nd isotopic data and REE abundances. *Geochim. Cosmochim. Acta* **54**, 1147–1154.
- Shirey S. B. and Walker R. J. (1998) The Re-Os system in cosmochemistry and high temperature geochemistry. *Ann. Revisions Earth Planet. Sci.* **26**, 423–500.
- Smith A. D. (2003) Critical evaluation of Re-Os and Pt-Os isotopic evidence on the origin of intraplate volcanism. *J. Geodynamics* **36**, 469–484.
- Smoliar M. I., Walker R. J., and Morgan J. W. (1996) Re-Os ages of group IIA, IIIA, IVA and IVB iron meteorites. *Science* **271**, 1099–1102.
- Snow J. E. and Schmidt G. (1998) Constraints on Earth accretion deduced from noble metals in the oceanic mantle. *Nature* **391**, 166–169.
- Stacey F. D. and Loper D. E. (1988) Thermal history of the Earth; a corollary concerning non-linear mantle rheology. *Phys. Earth Planet. Interiors* **53**, 167–174.
- Steiger R. H. and Jäger E. (1977) Subcommission on geochronology: Convention on the use of decay constants in geo- and cosmochronology. *Earth Planet. Sci. Lett.* **1**, 369–371.
- Stern R. J., Morris J., Bloomer S. H., and Hawkins J. W. (1991) The source of subduction component in convergent margin magmas: Trace element and radiogenic evidence from Eocene boninites, Mariana fore arc. *Geochim. Cosmochim. Acta* **55**, 1467–1481.
- Sun S.-S. (1987) Chemical composition of Archean komatiites: Implications for early history of the earth and mantle evolution. *J. Volcanol. Geothermal Res.* **32**, 67–82.
- Sun S.-S. and McDonough W. F. (1989) Chemical and isotopic systematics of oceanic basalts: Implications for mantle compositions and processes. In *Magmatism in the Ocean Basins* (eds. A. D. Saunders and M. J. Norry), pp. 313–345. Geological Society Special Publication 42, Geological Society of London.
- Taylor R. N., Nesbitt R. W., Vidal P., Harmon R. S., Auvray B., and Croudace I. W. (1994) Mineralogy, chemistry, and genesis of the boninite series volcanics, Chichijima, Bonin Islands, Japan. *J. Petrol.* **35**, 577–617.
- Todt W., Cliff R. A., Hanser A., and Hofmann A. W. (1993) Recalibration of NBS lead standards using a  $^{202}\text{Pb} + ^{205}\text{Pb}$  double spike. *Terra Abstr.* **5** (Suppl. 1), 396.
- Walker D. (2000) Core partitioning in mantle geochemistry: Geochemical Society Ingerson Lecture, GSA Denver, October 1999. *Geochim. Cosmochim. Acta* **64**, 2897–2911.
- Walker R. J., Morgan J. W., and Horan M. F. (1995) Osmium-187 enrichment in some plumes: Evidence for core-mantle interaction? *Science* **269**, 819–822.
- Walker R. J. and Nisbet E. (2002)  $^{187}\text{Os}$  isotopic constraints on Archean mantle dynamics. *Geochim. Cosmochim. Acta* **66**, 3317–3325.
- Walker R. J., Prichard H. M., Ishiwatari A., and Pimentel M. (2002) The osmium isotopic composition of convecting upper mantle deduced from ophiolite chromites. *Geochim. Cosmochim. Acta* **66**, 329–345.
- Wilson A. H., Shirey S. B., and Carlson R. W. (2003) Archean ultra-depleted komatiites formed by hydrous melting of cratonic mantle. *Science* **423**, 858–861.

**Appendix.** Locations of some “least altered” boninite-like metabasalts from within the northeast central tectonic domain of the ISB.

|       | 462901      | 462904     | 462945     | 462946     | 462948     | 462949     | 462965*    | 462967     | 462903     | 462906     | 462947     | 462966     | 462902     |
|-------|-------------|------------|------------|------------|------------|------------|------------|------------|------------|------------|------------|------------|------------|
| North | 65°.10.65°0 | 65°.10.802 | 65°.10.368 | 65°.10.368 | 65°.10.368 | 65°.10.368 | 65°.11.139 | 65°.11.163 | 65°.10.806 | 65°.11.034 | 65°.10.368 | 65°.11.311 | 65°.10.726 |
| West  | 49°.47.49°5 | 49°.47.259 | 49°.49.364 | 49°.49.364 | 49°.49.364 | 49°.49.364 | 49°.47.373 | 49°.49.962 | 49°.47.347 | 49°.46.878 | 49°.49.364 | 49°.47.668 | 49°.47.474 |